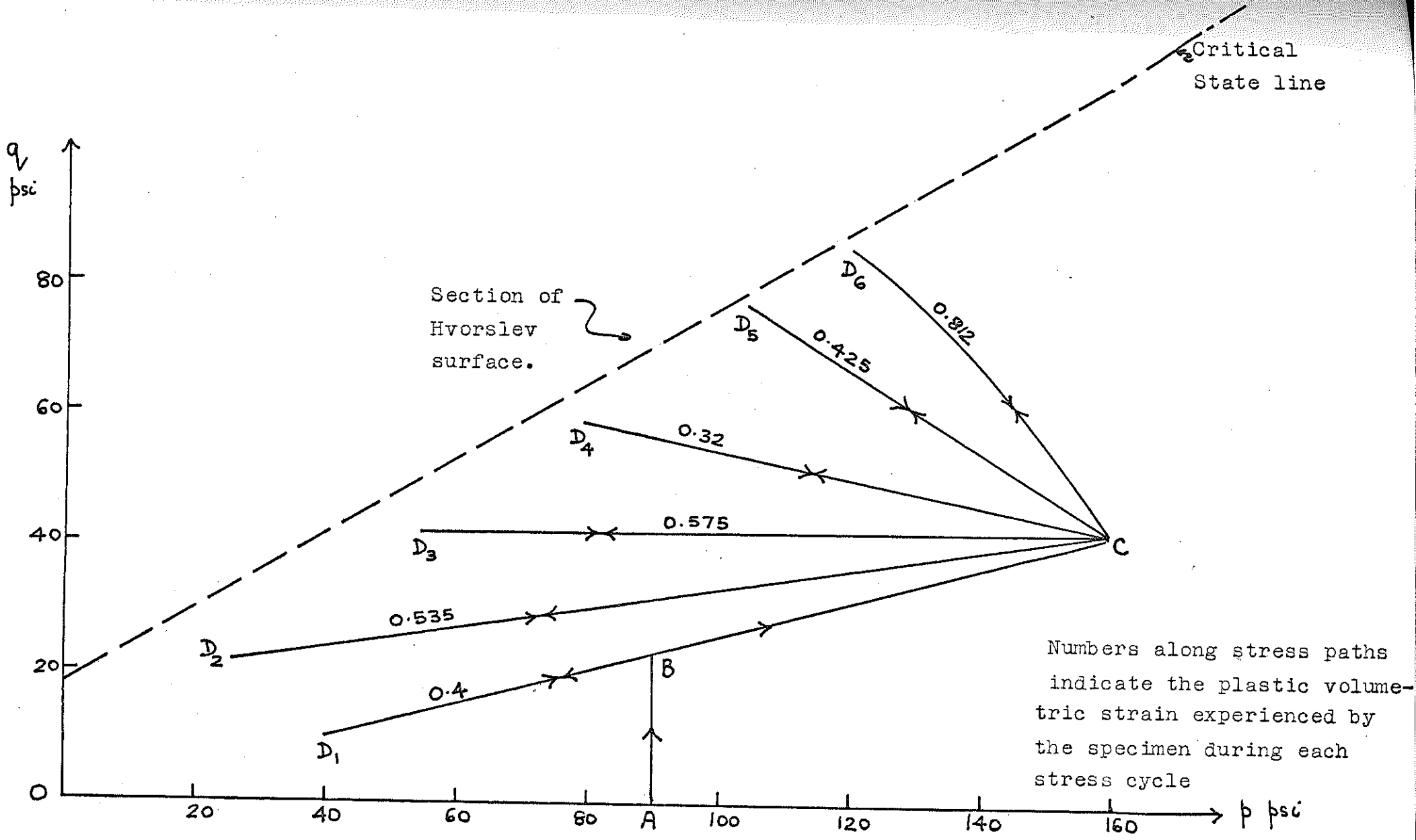

Fig. 6.2(d). The plastic volumetric strain experienced by specimen CF during stress cycles CD_IC, CD_2C, etc.

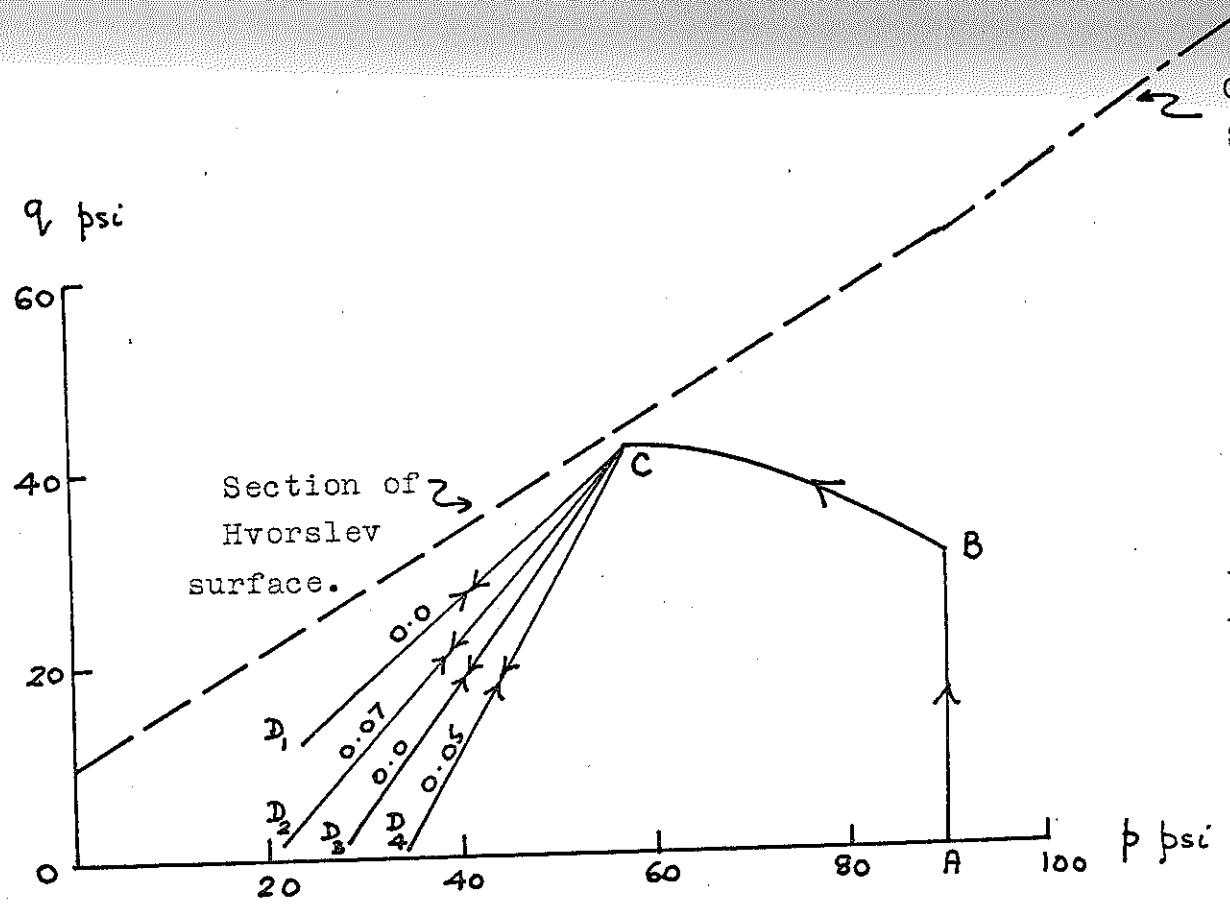

Numbers along stress paths indicate the plastic volumetric strain experienced by the specimen during each stress cycle.

Fig. 6.2(e). The plastic volumetric strain experienced by specimen T_{I6} during stress cycles CD_IC, CD_2C, ETC.

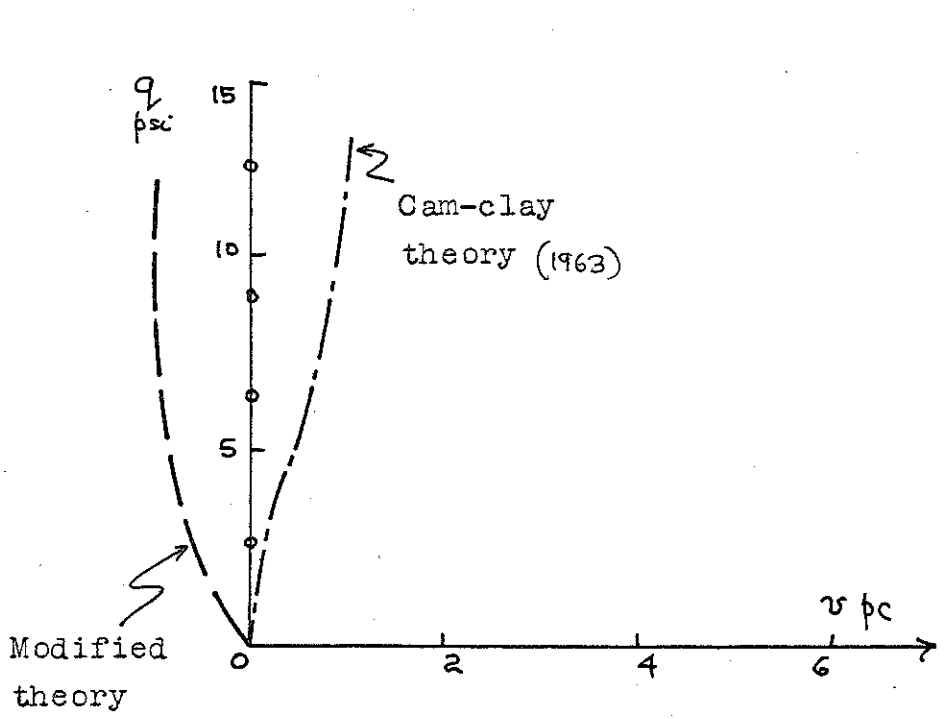

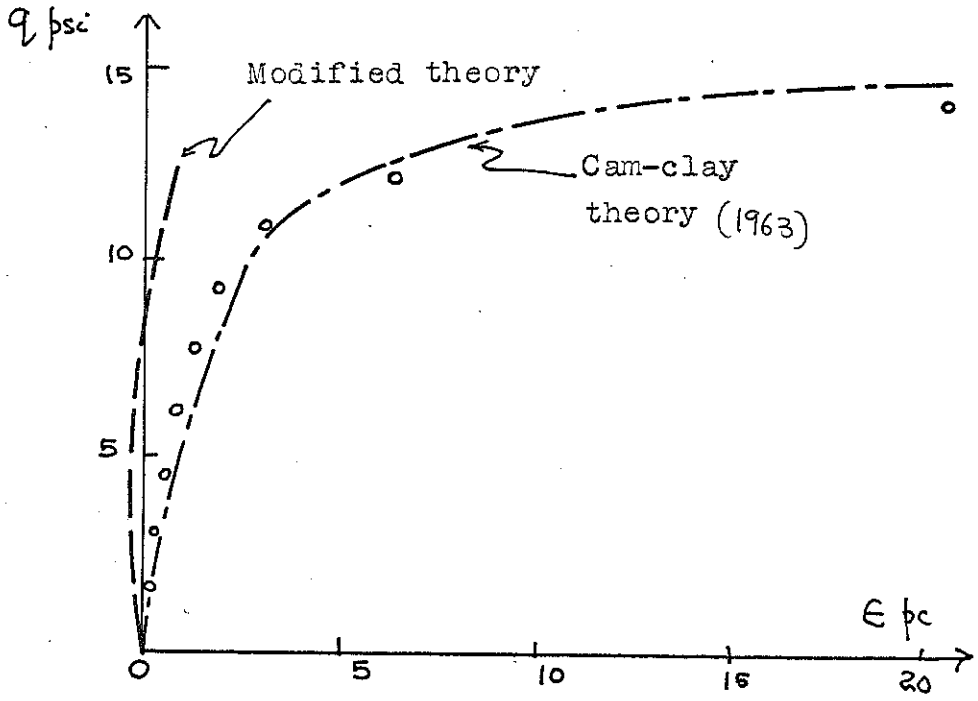

Fig. 6.3. Observed and predicted strains for an experimentally observed undrained stress path from 30 psi isotropic stress.

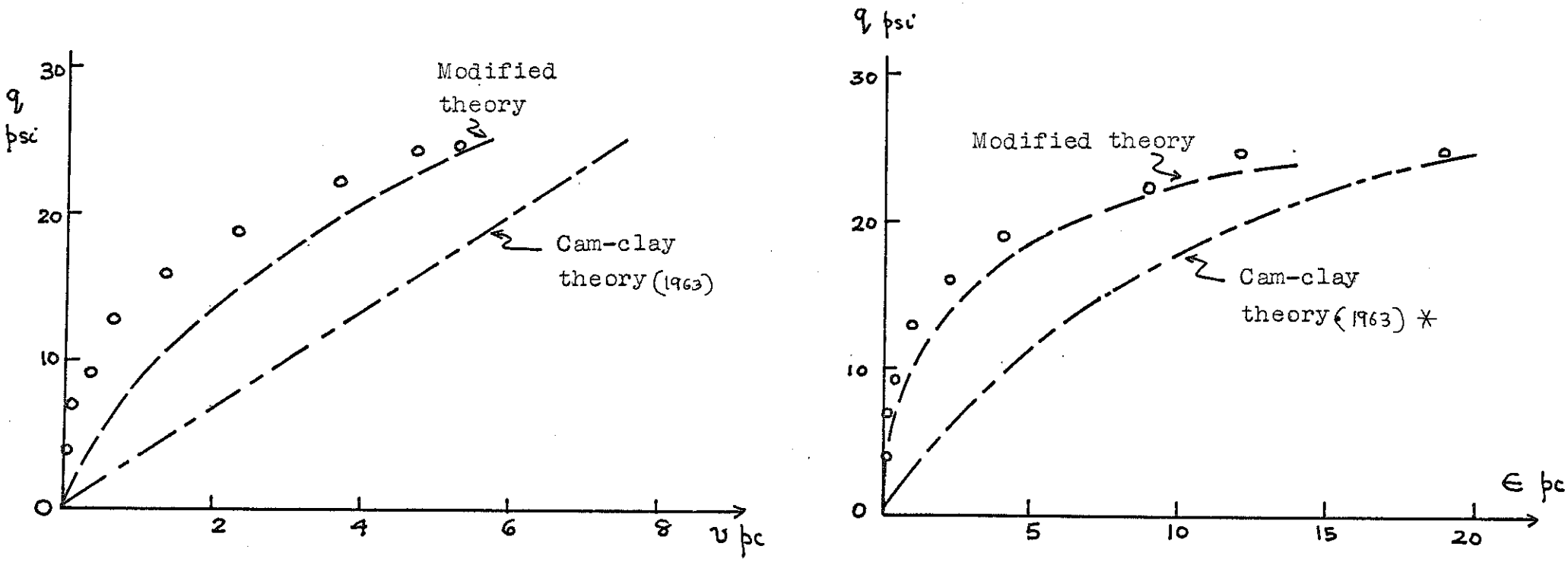

Fig. 6.4. Observed and predicted strains for a constant p test from 30 psi isotropic stress.

* Schofield and Wroth (1968) adapted a different method to that employed by the Author for obtaining the fundamental soil constants. As a consequence their "Cam clay" predicted strains will be different from those presented by the Author in this dissertation.

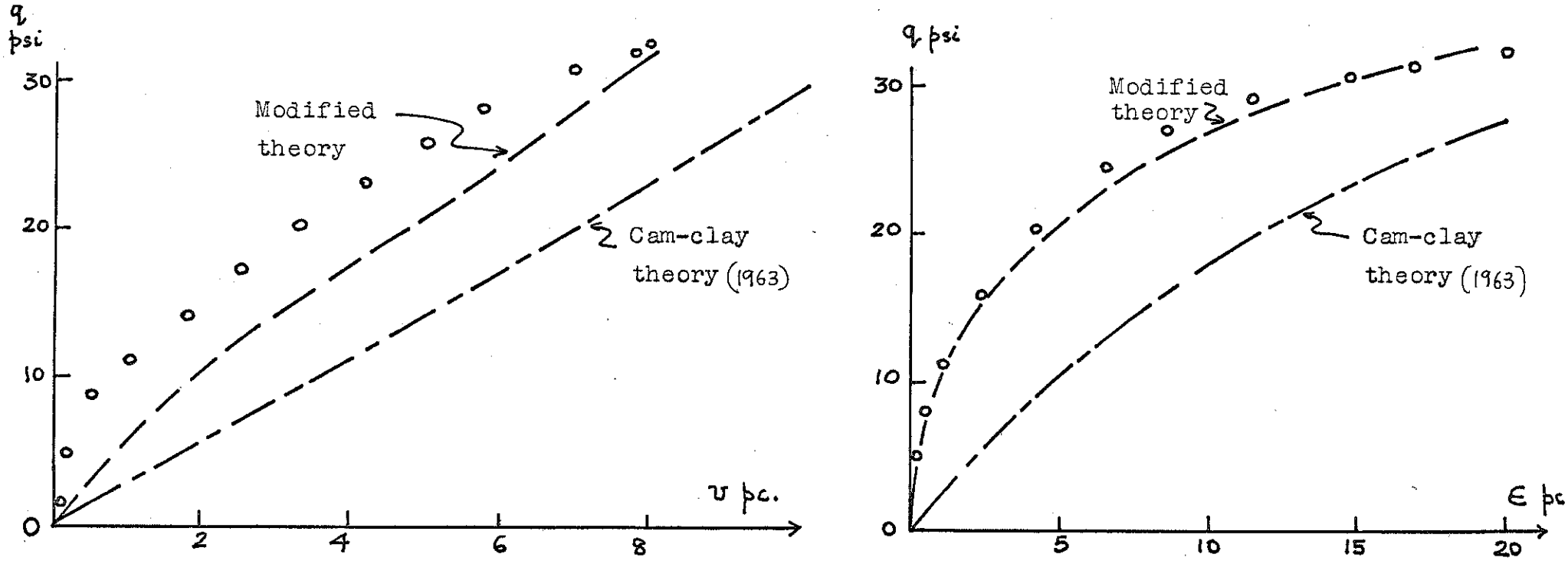

Fig. 6.5. The observed and predicted strains for a fully drained test from 30 psi isotropic stress with constant cell pressure.

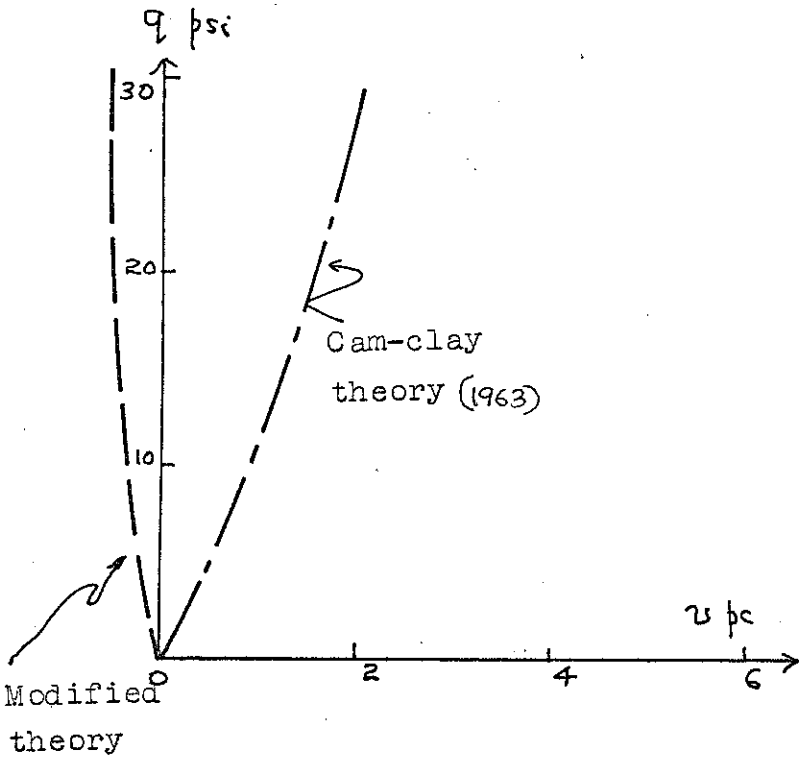

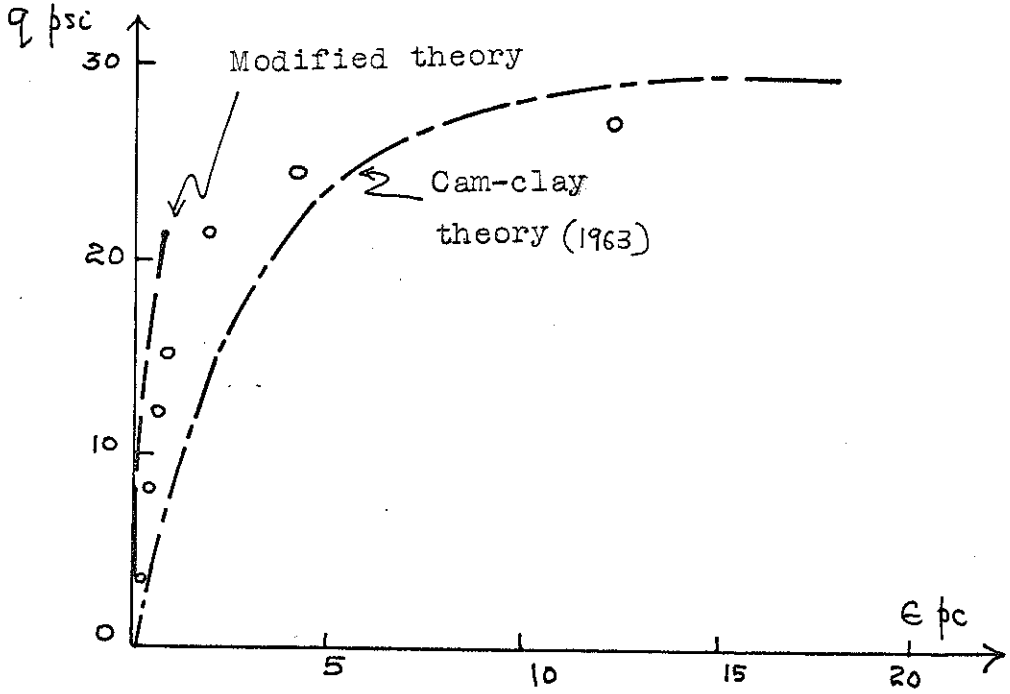

Fig. 6.6. Observed and predicted strains for an experimentally observed undrained stress path from 60 psi isotropic stress.

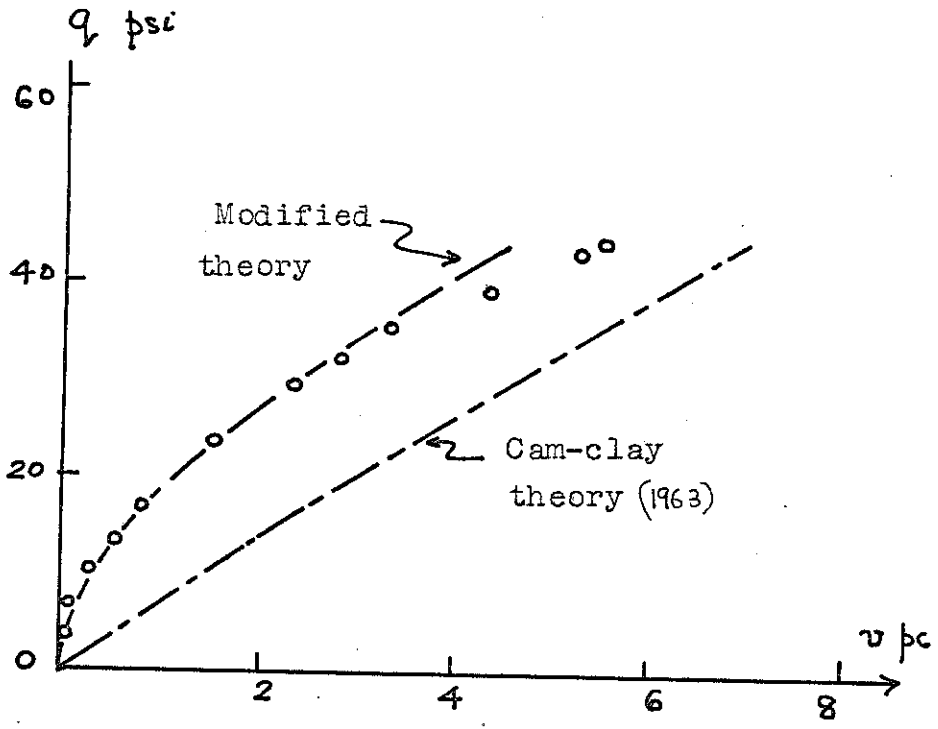

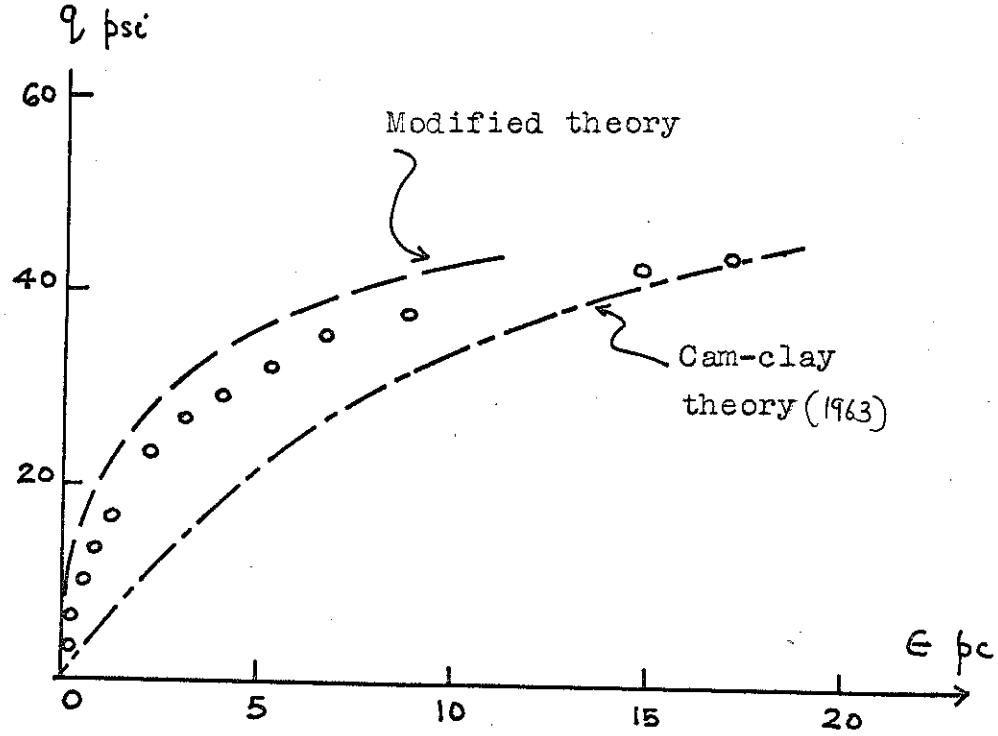

Fig. 6.7. Observed and predicted strains for a constant p test from 60 psi isotropic stress.

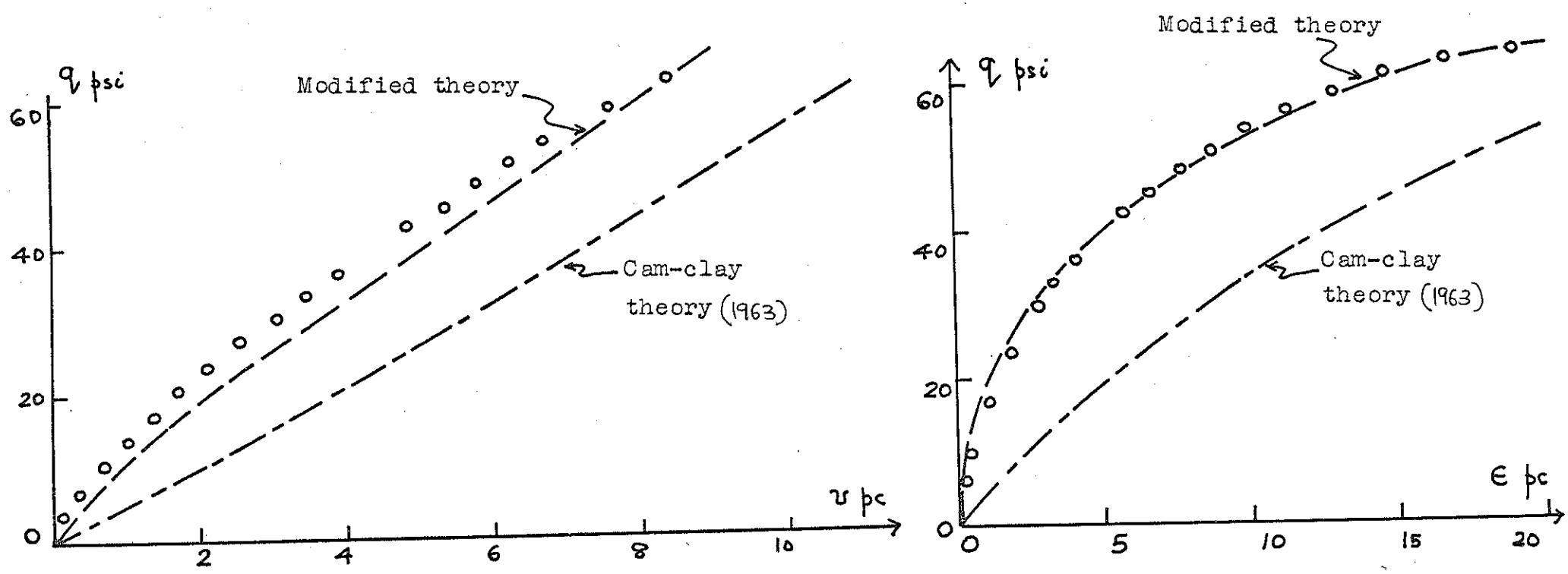

Fig. 6.8. Observed and predicted strains for a fully drained test from 60 psi isotropic stress with constant cell pressure.

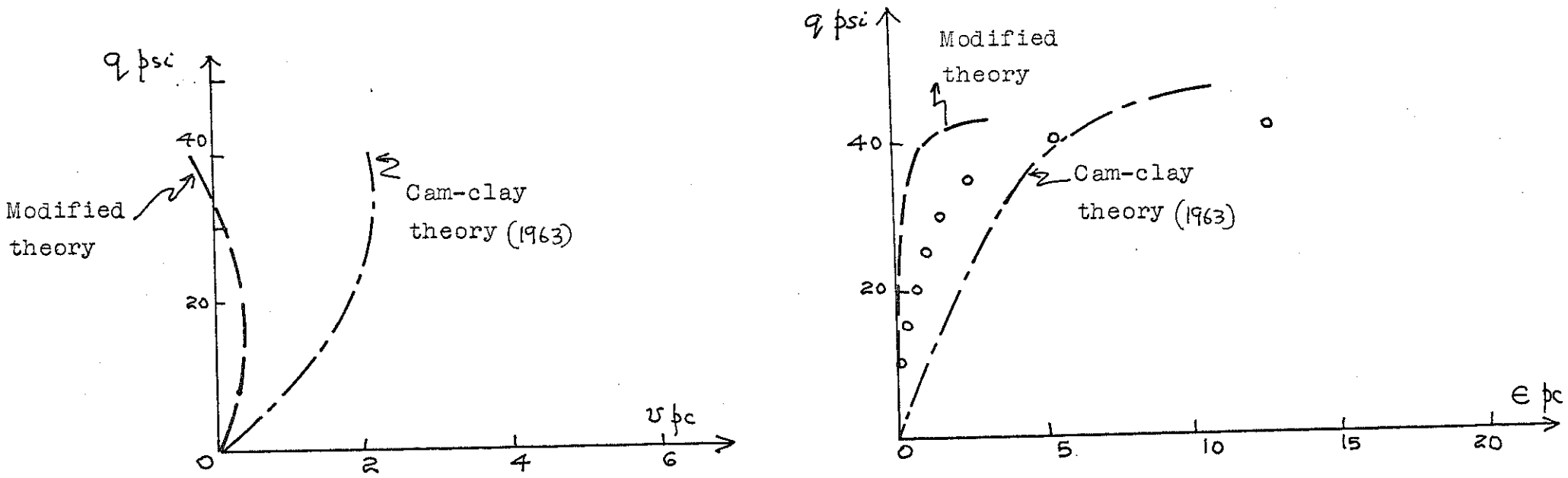

Fig. 6.9. Observed and predicted strains for an experimentally observed undrained stress path from 90 psi isotropic stress.

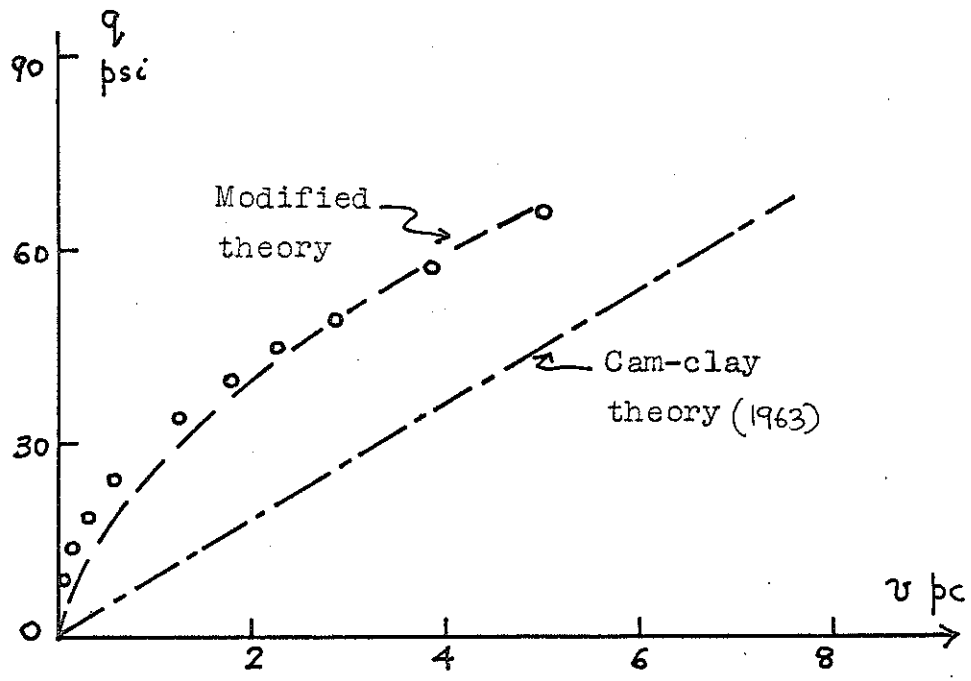

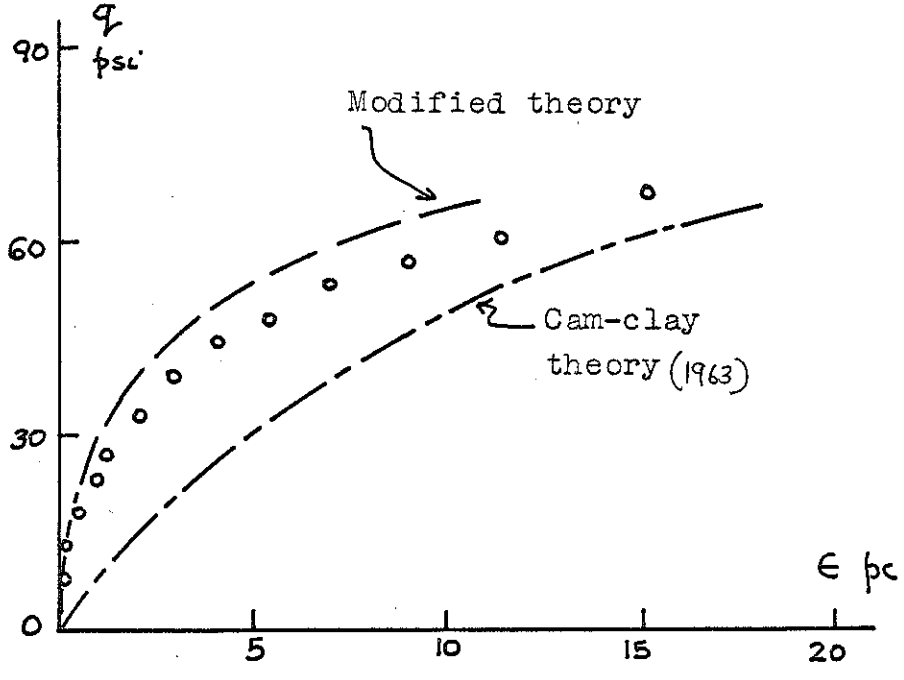

Fig. 6.10. Observed and predicted strains for a constant p test from 90 psi isotropic stress.

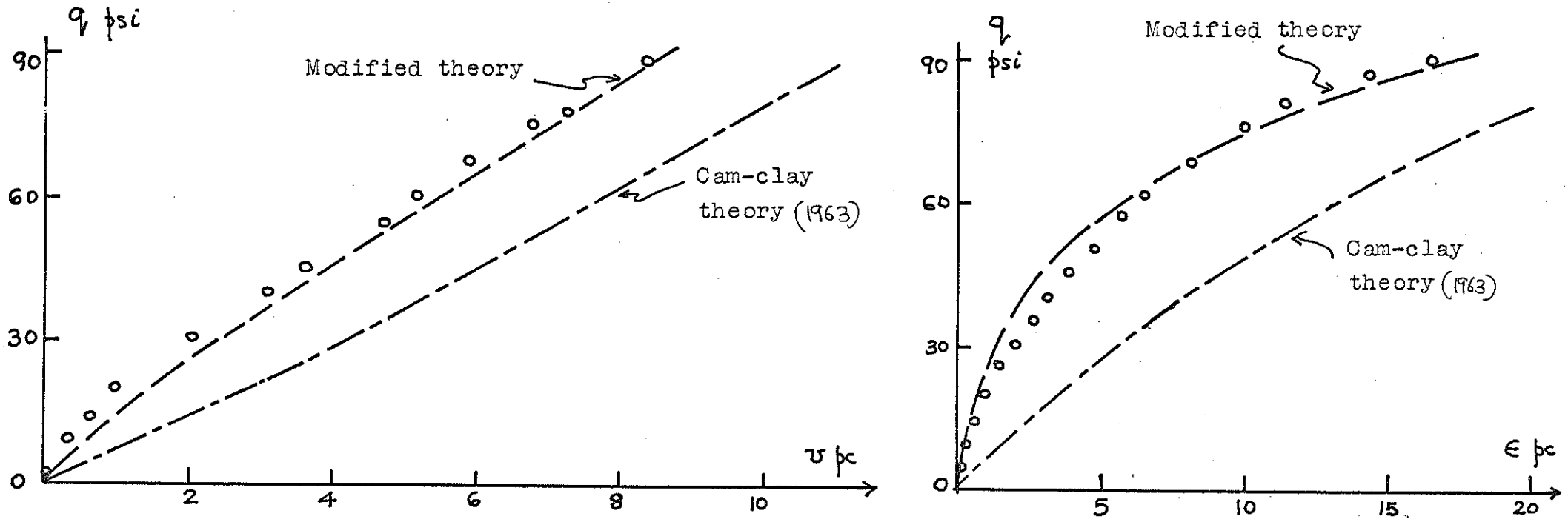

Fig. 6.11. Observed and predicted strains for a fully drained test from 90 psi isotropic stress with constant cell pressure.

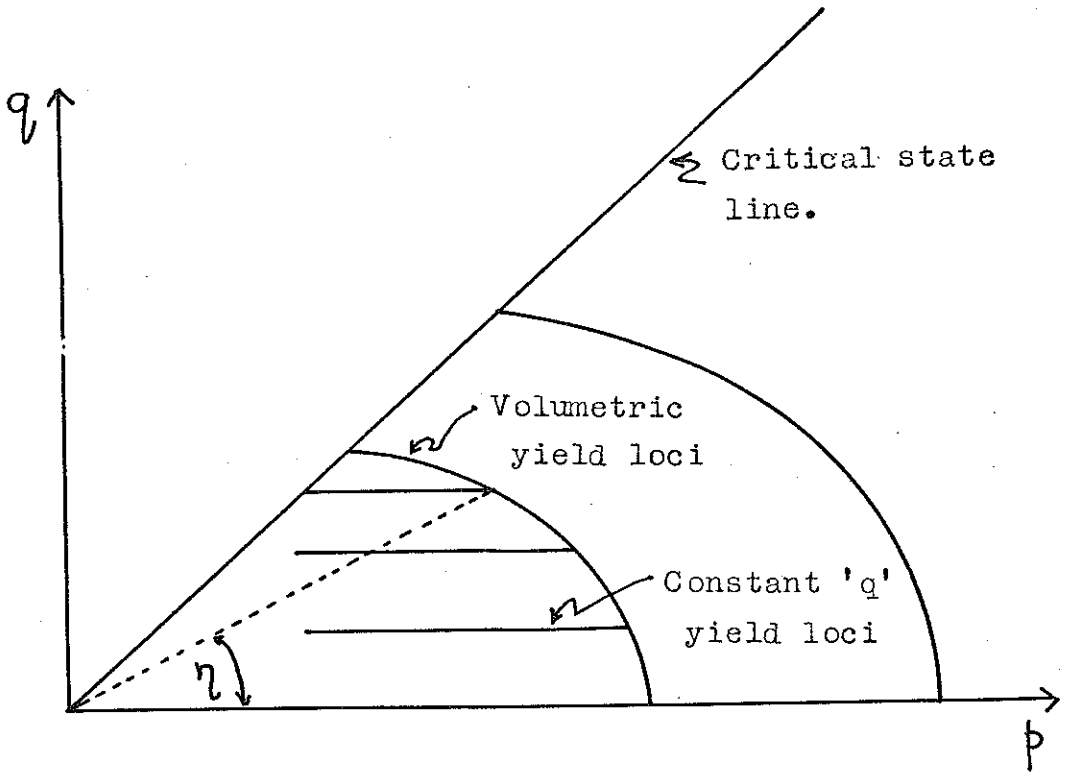

Fig. 6.12. Volumetric and constant 'q' yield loci of Roscoe and Burland (1968).

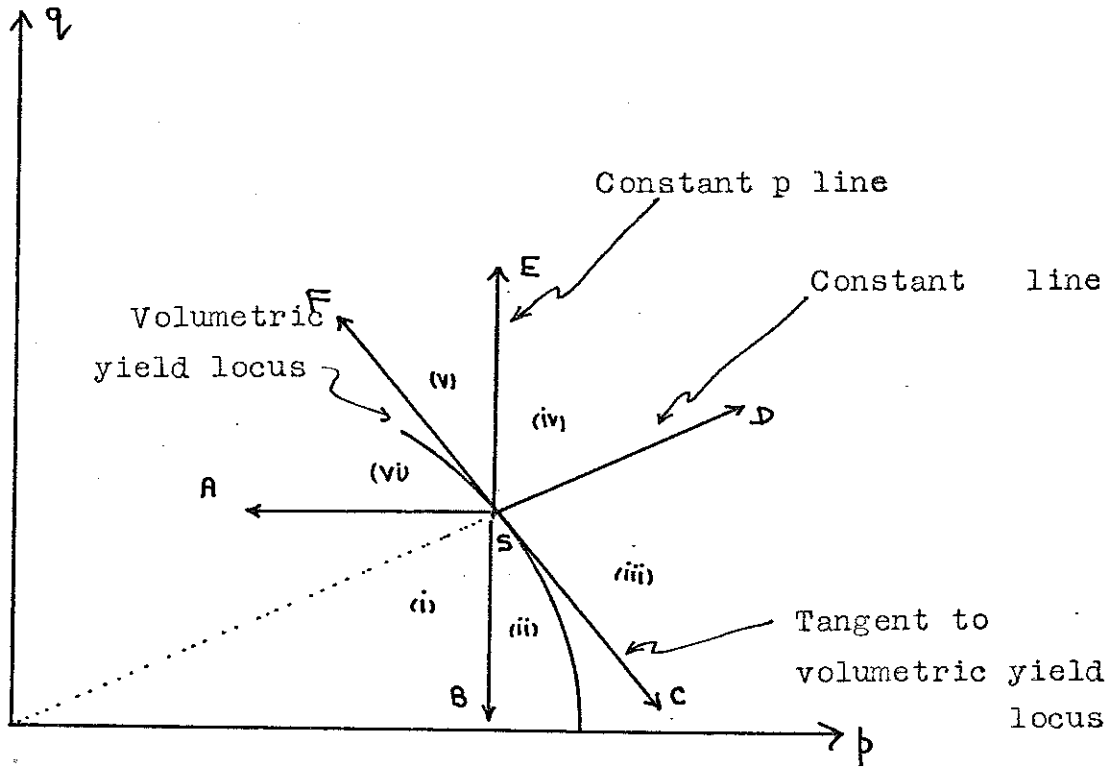

Fig. 6.I2(a) Division of stress plane to describe the incremental stress strain relationships of Roscoe and Burland (I968)

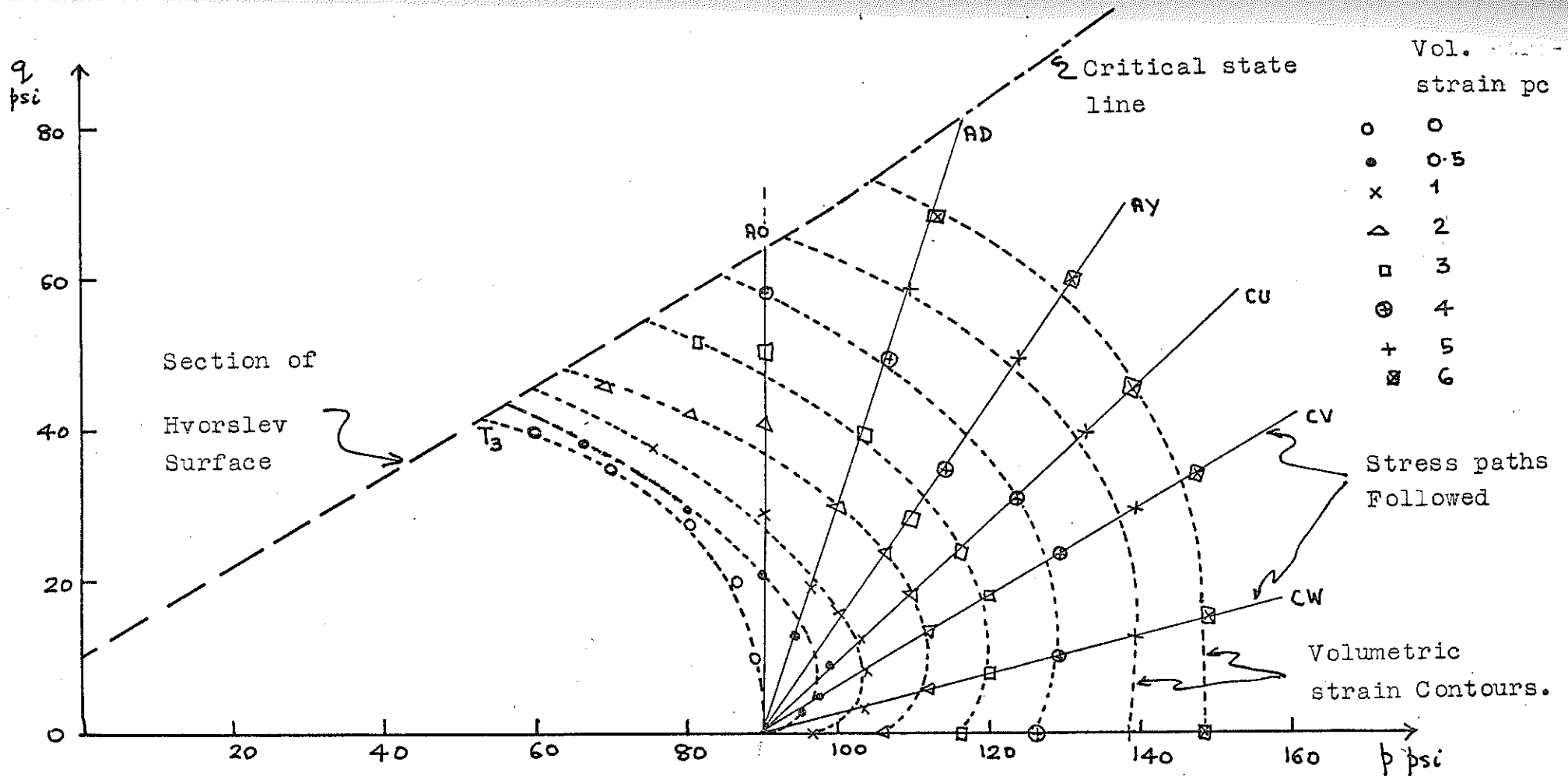

Fig. 6·13. Volumetric strain contours obtained from a variety of drained tests (each with constant dq/dp) and the zero volumetric strain contour from an undrained test.

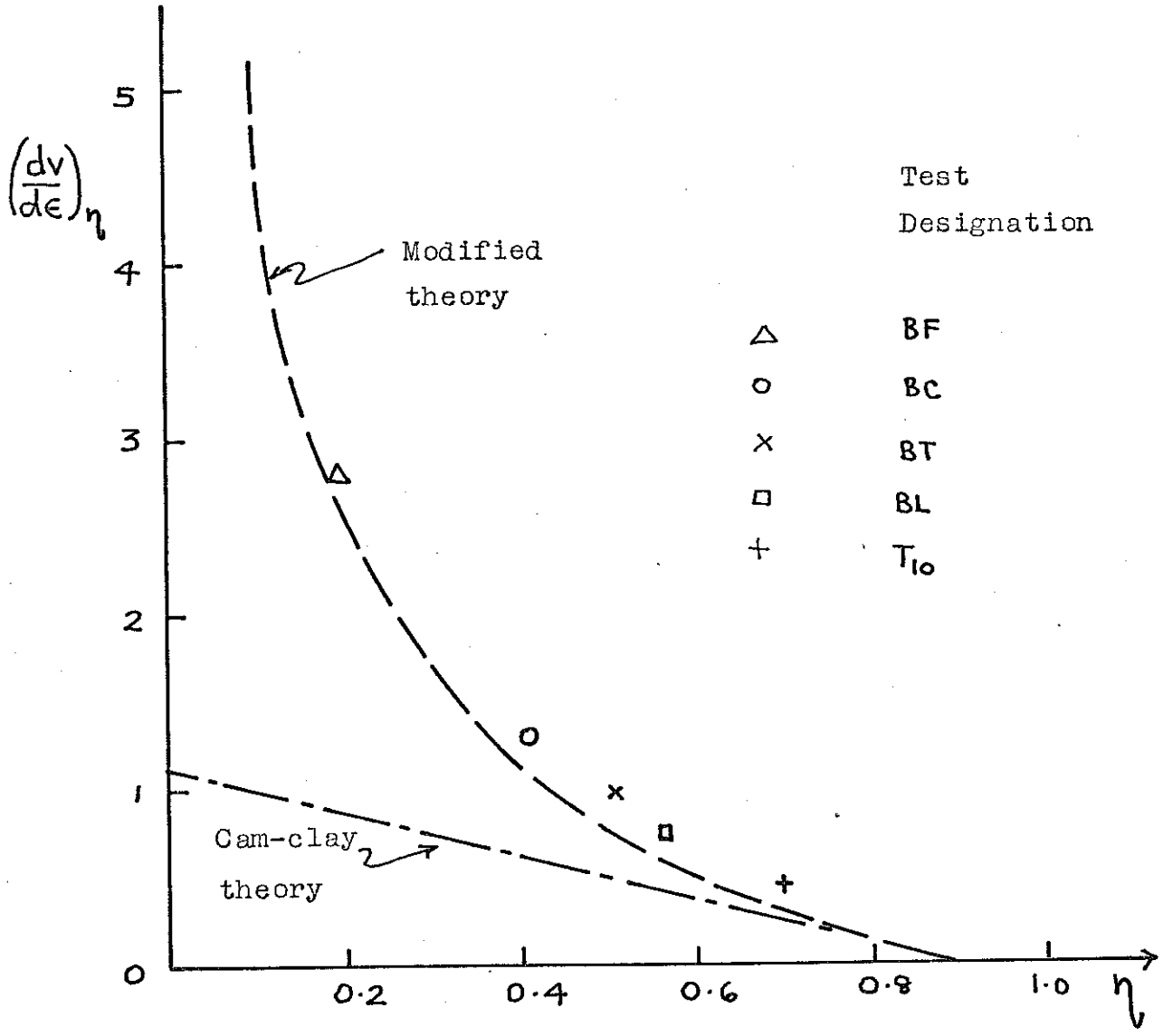

Fig. 6.14. Observed and predicted $\left(\left(\frac{dv}{d\epsilon}\right)_\eta, \eta\right)$ relationship for anisotropic consolidation tests.

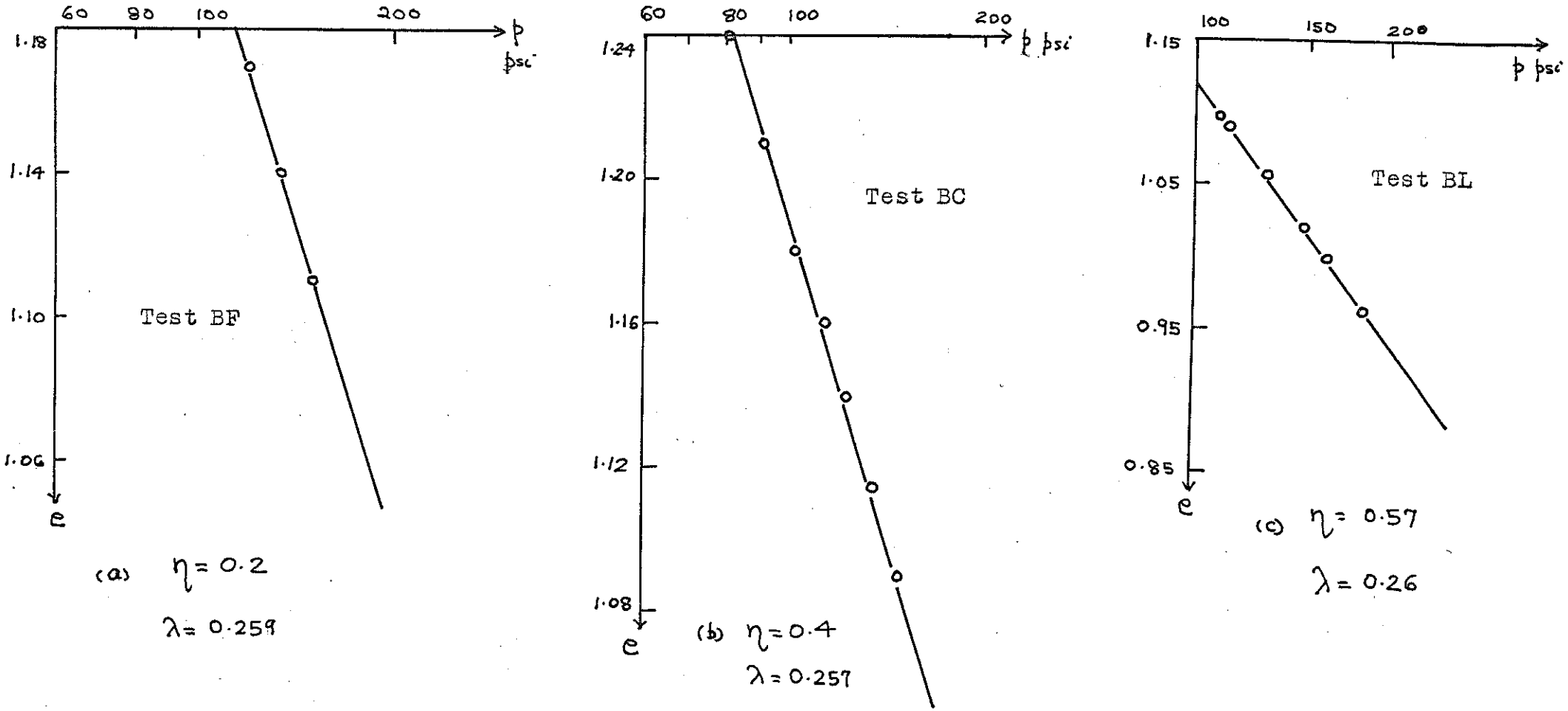

Fig. 6.14(a-c) The (e, log p) characteristics for anisotropic consolidation tests.

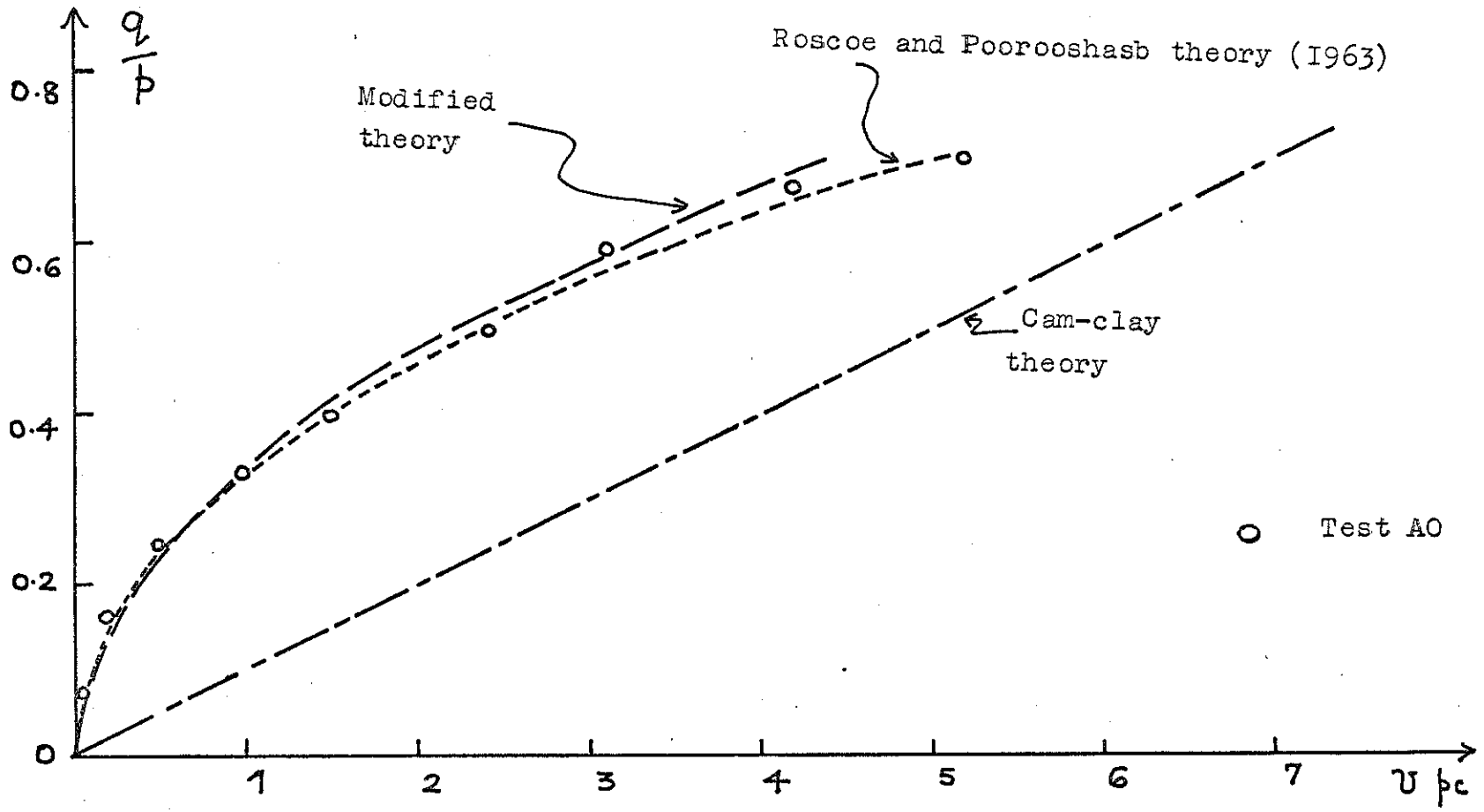

Fig. 6.15. Observed and predicted $(\frac{q}{p}, \upsilon)$ relationship for a constant p test from 90 psi isotropic stress.

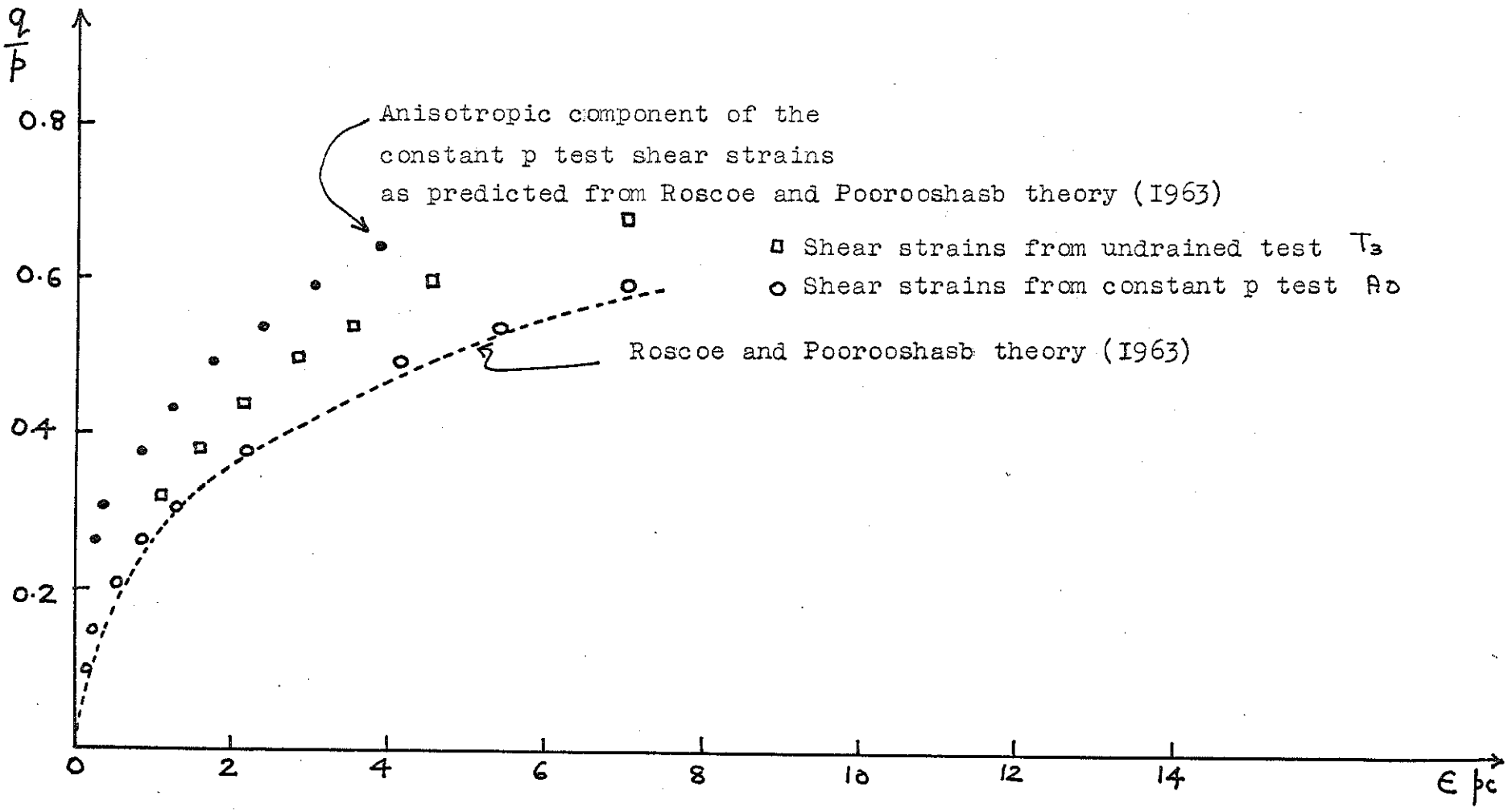

Fig. 6.16(a). Observed and predicted strains for a constant p test from 90 psi isotropic stress.

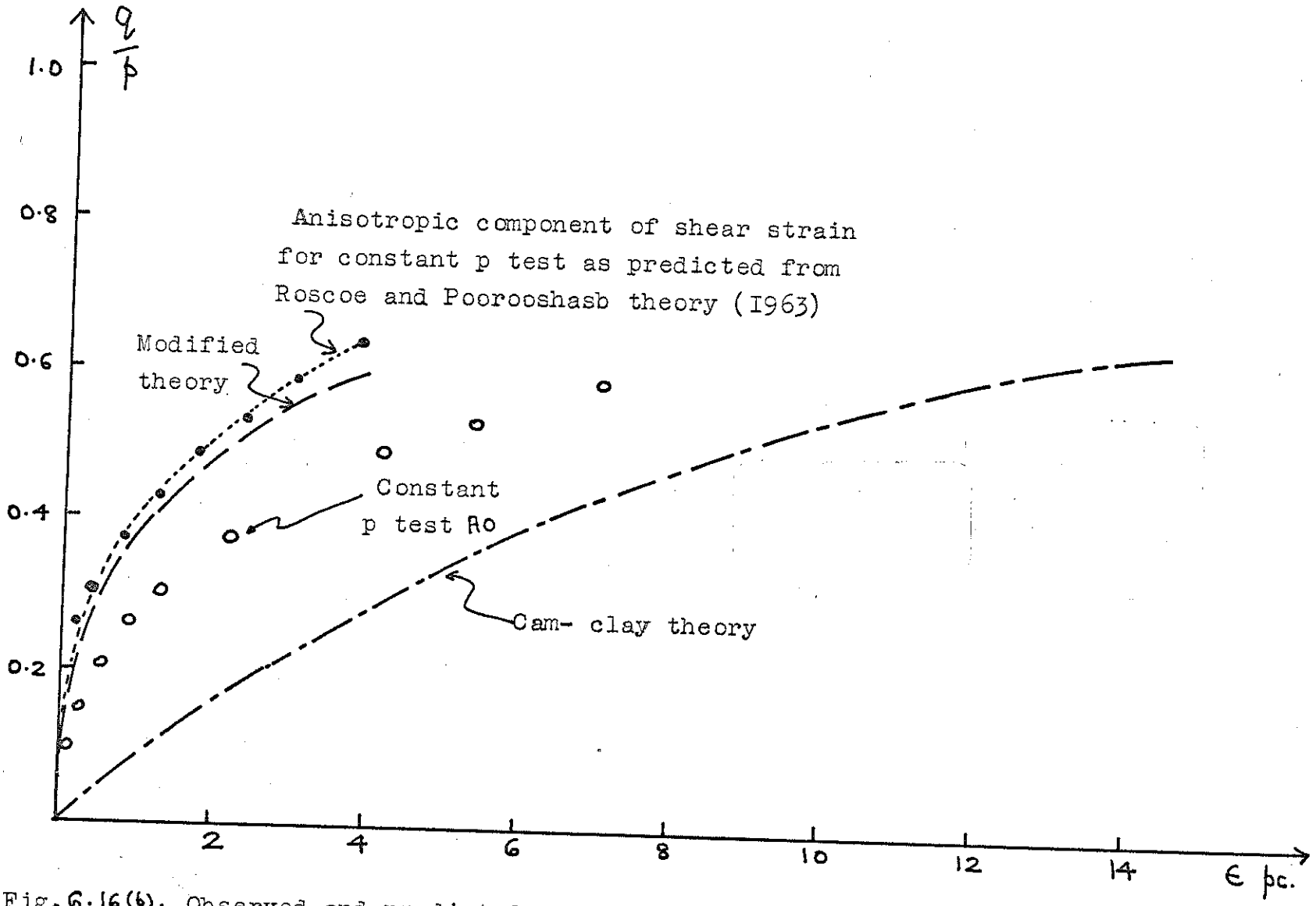

Fig. 6.16(6). Observed and predicted strains for a constant p test from 90 psi isotropic stress.

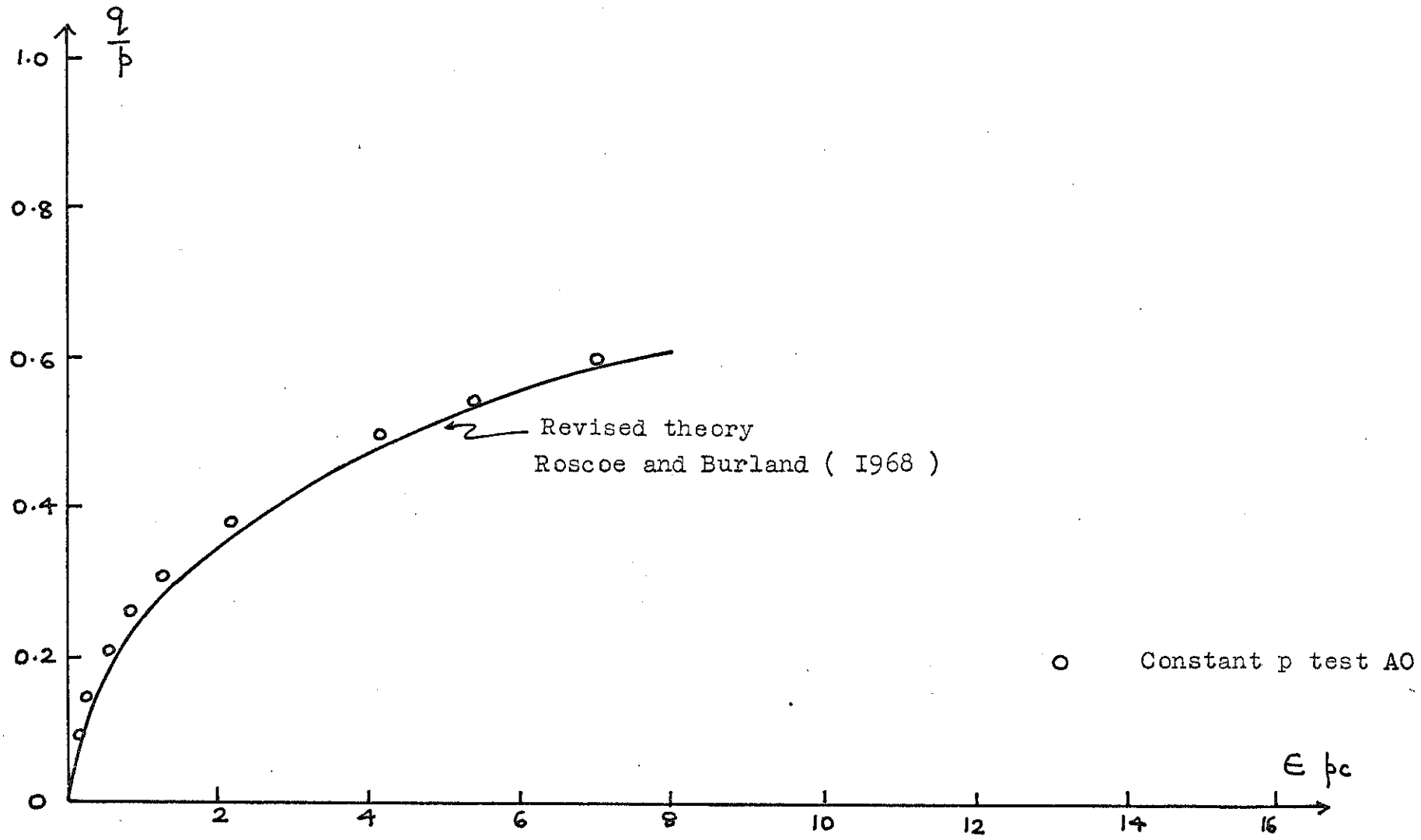

Fig.6.17. Observed and predicted $(\frac{q}{p}, \varepsilon)$ relationship for a constant p test from 90 psi isotropic stress.

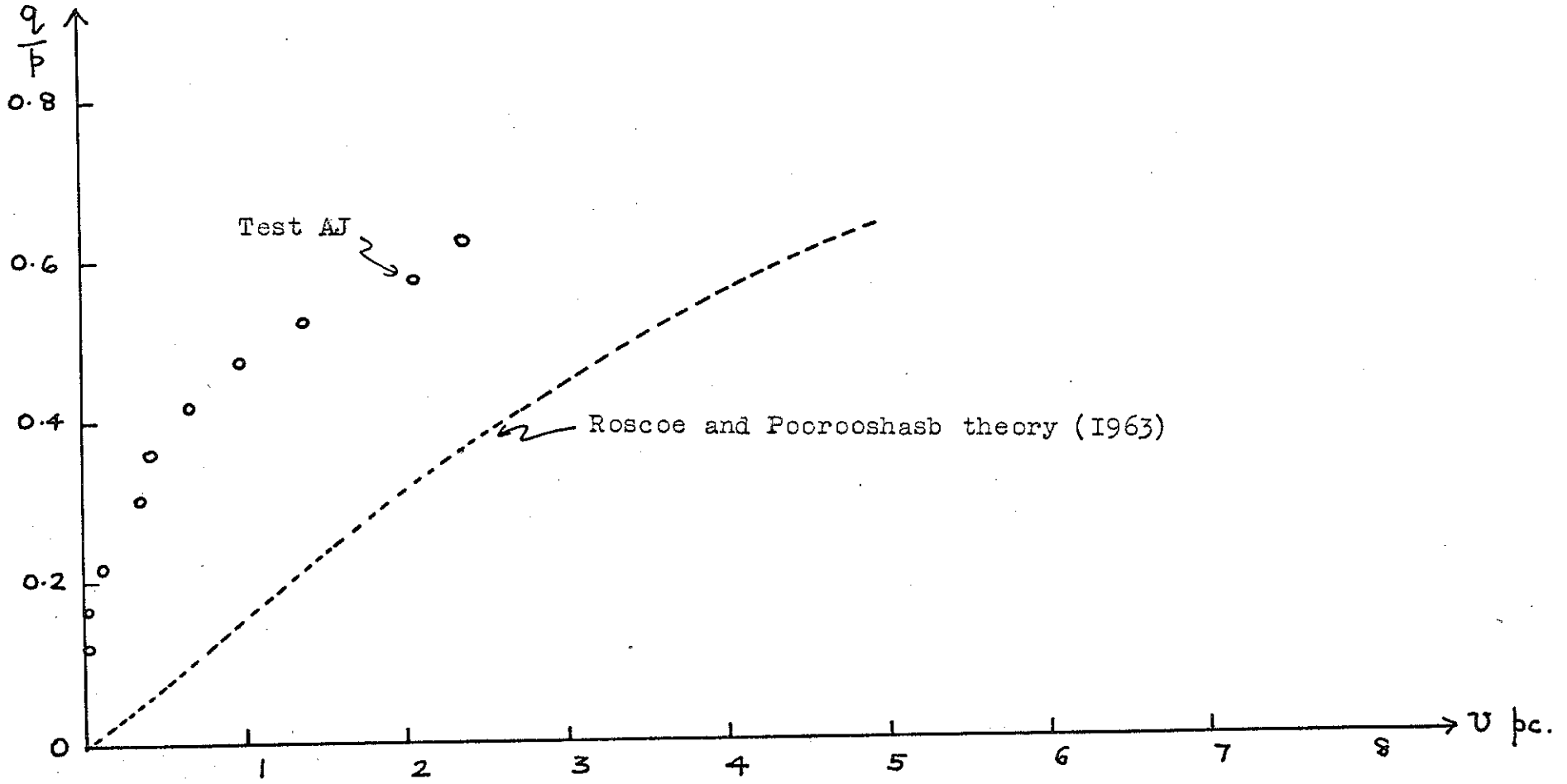

Fig. 6·18. Observed and predicted strains for a constant p test from 30 psi isotropic stress.

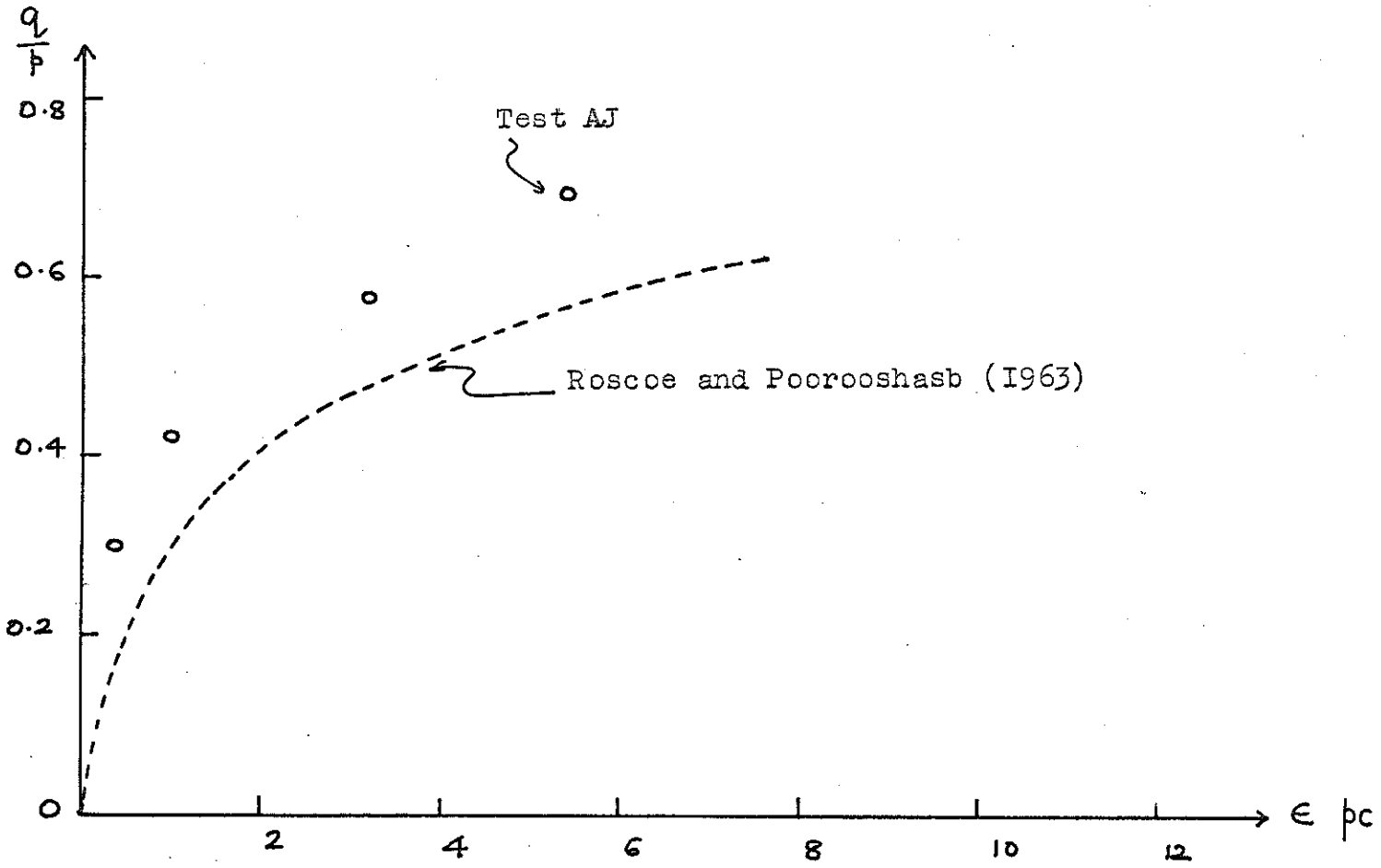

Fig. 6.19 Observed and predicted ($\frac{q}{p}$, ϵ) relationship for a constant p test from 30 psi isotropic stress

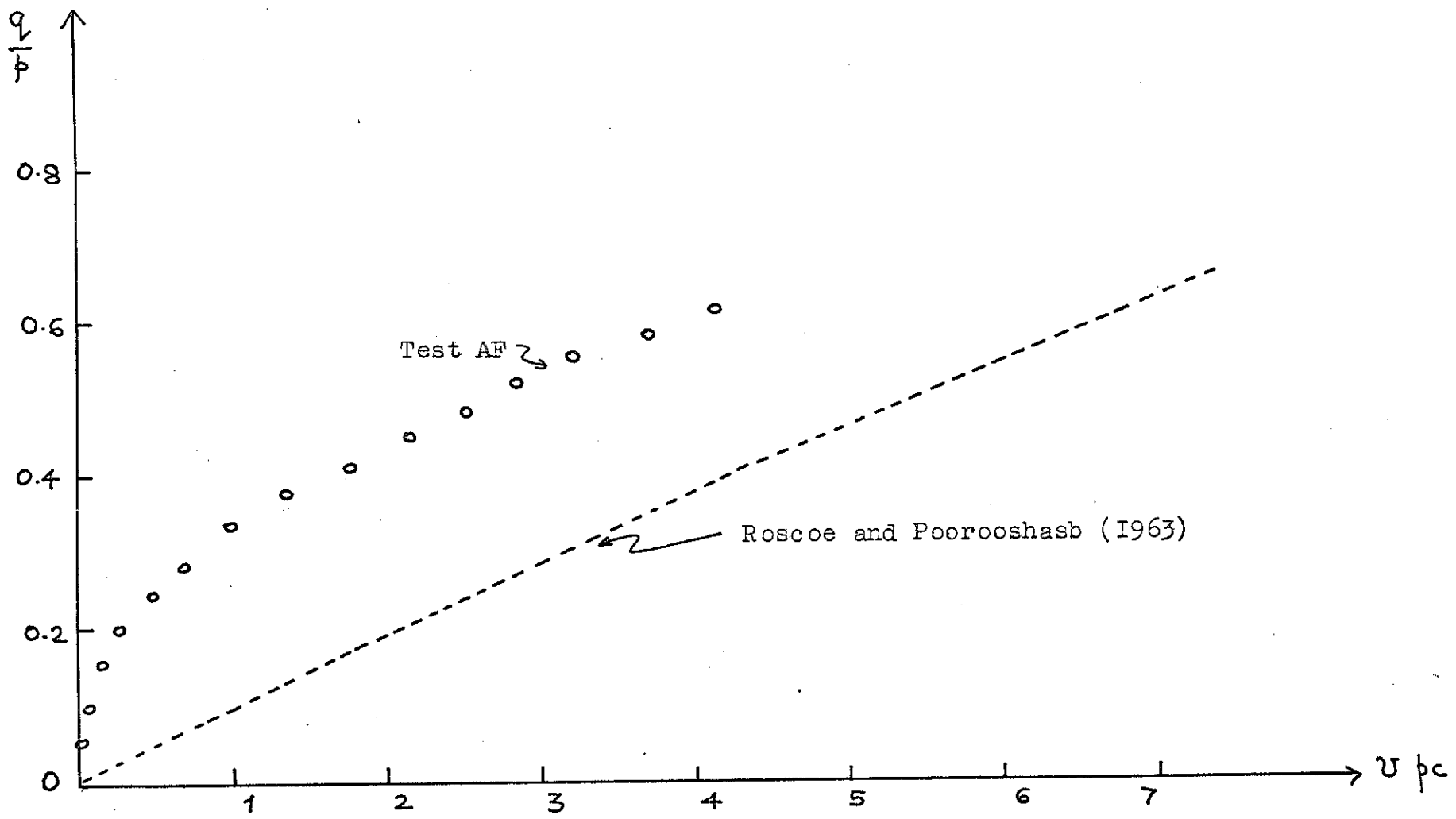

Fig. 6.20. Observed and predicted ($\frac{q}{p}$, υ) relationship for a fully drained test at 30 psi isotropic stress with constant cell pressure.

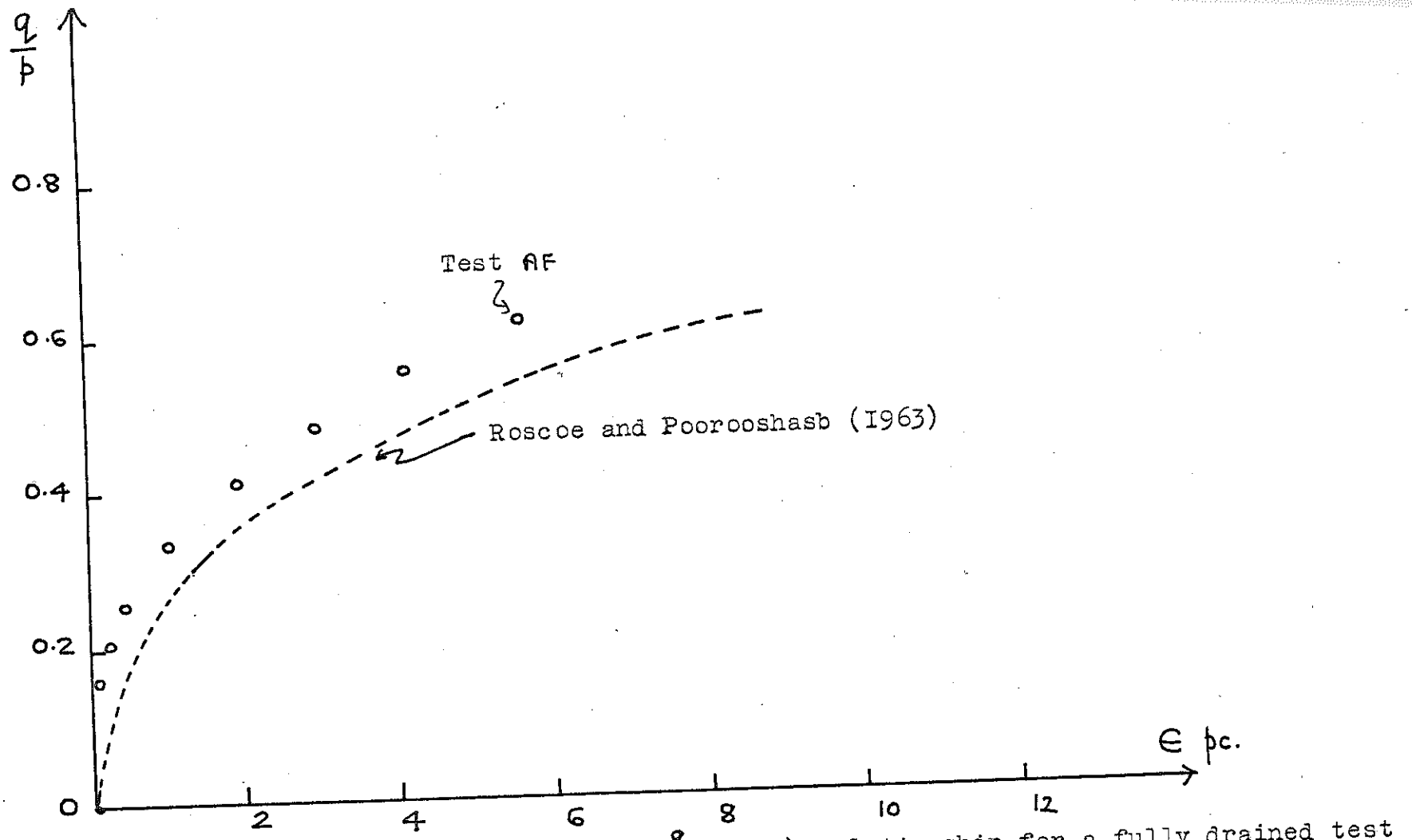

Fig. 6.21 Observed and predicted (q/p, ϵ) relationship for a fully drained test from 30 psi isotropic stress with constant cell pressure.

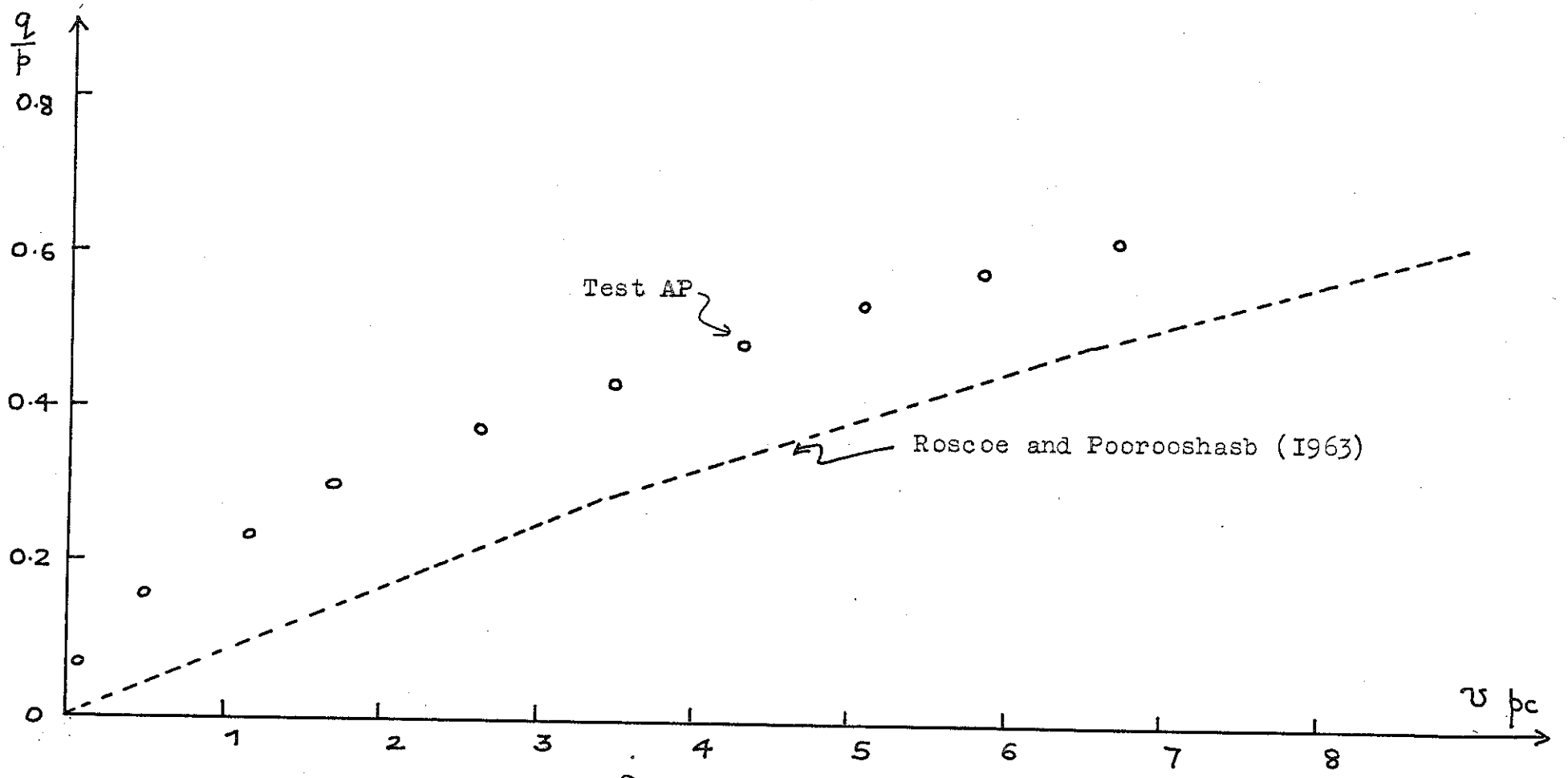

Fig. 6.22. Observed and predicted ($\frac{q}{p}$, v) relationship for a drained test from 30 psi isotropic stress with applied stress path of slope 2.

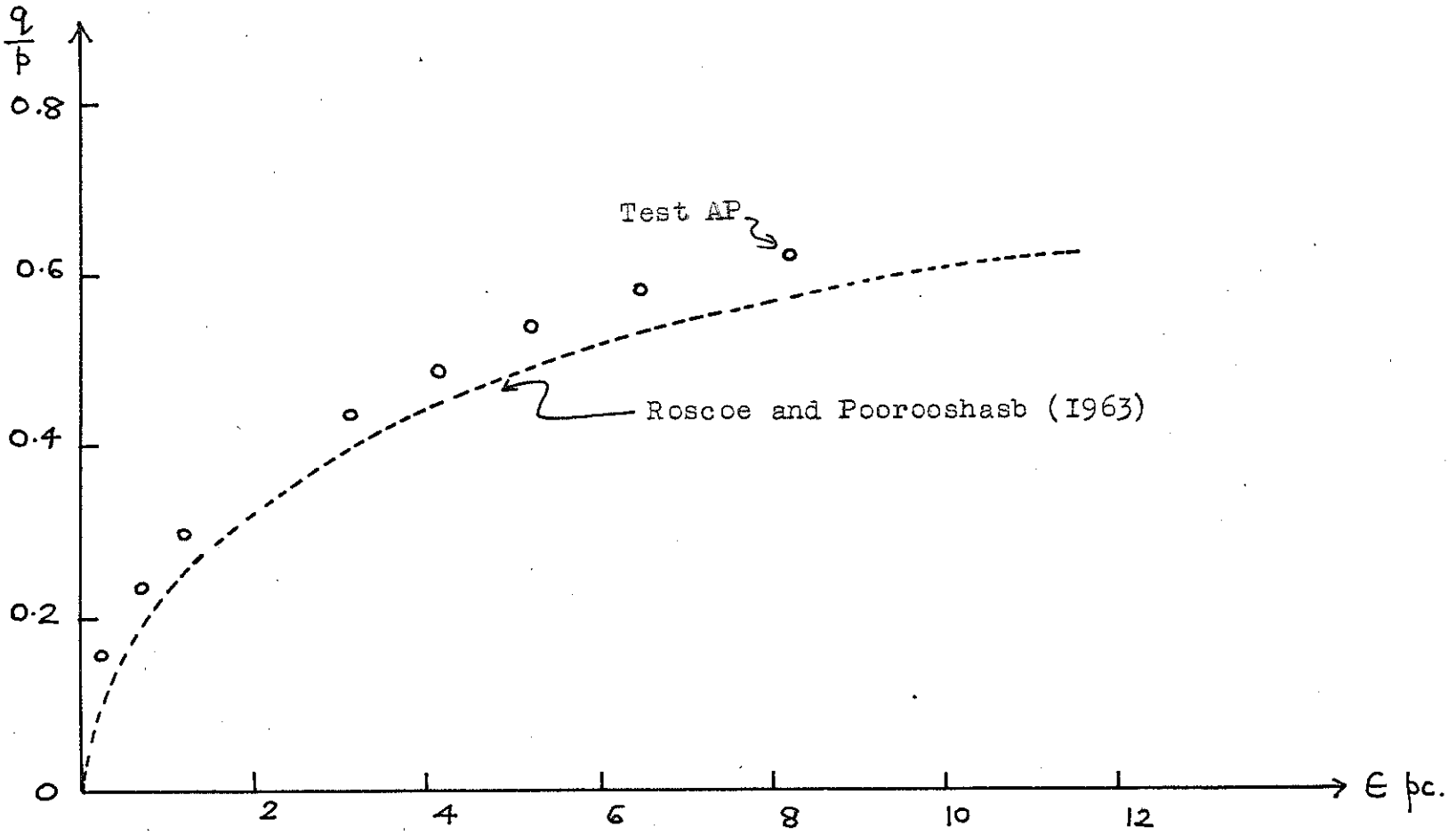

Fig. 6.23. Observed and predicted ($\frac{q}{p}$, ϵ) relationship for a drained test from 30 psi isotropic stress with an applied stress path of slope 2.

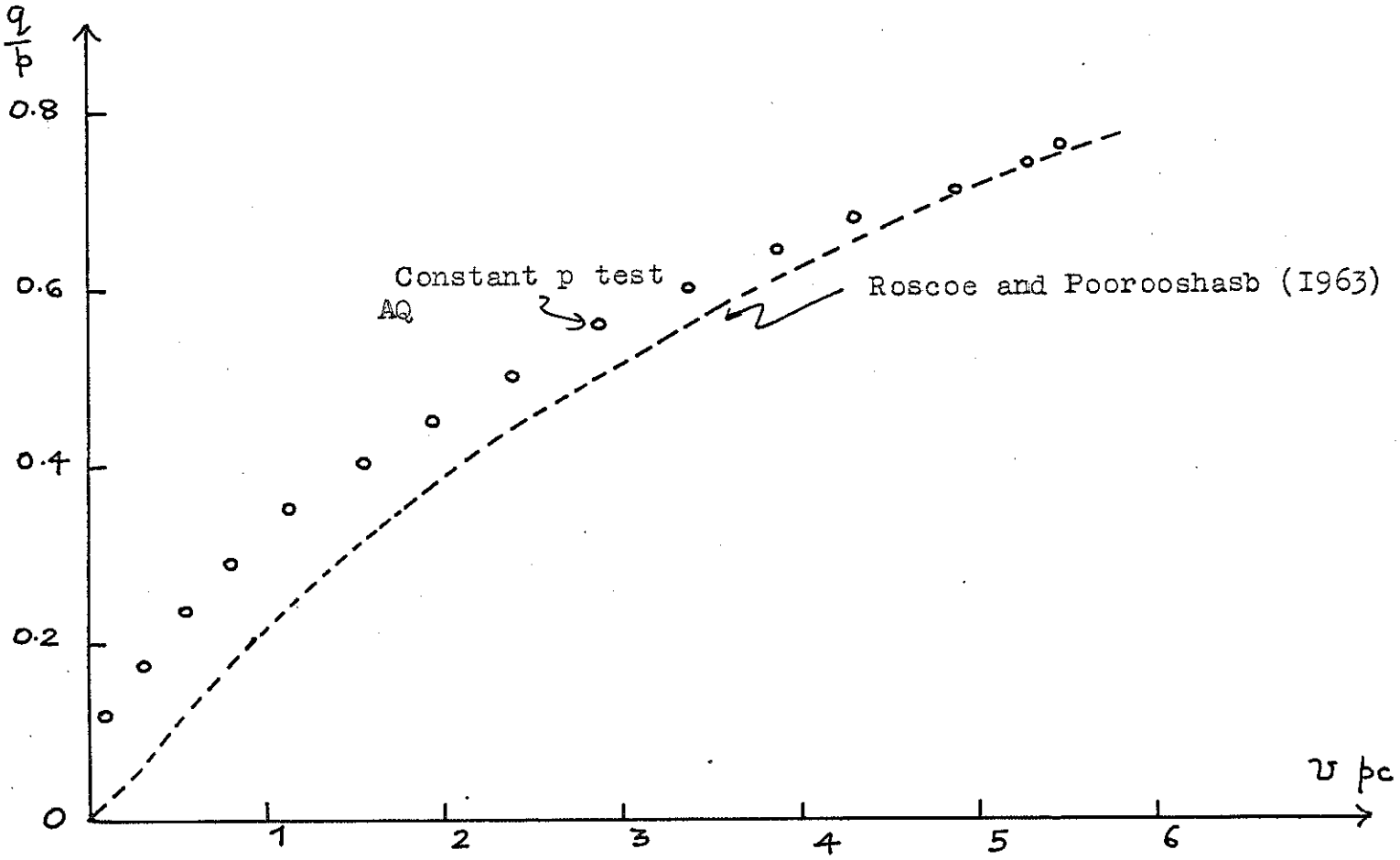

Fig. 6.24. Observed and predicted $(\frac{q}{p}, \upsilon)$ relationship for a constant p test from 60 psi isotropic stress.

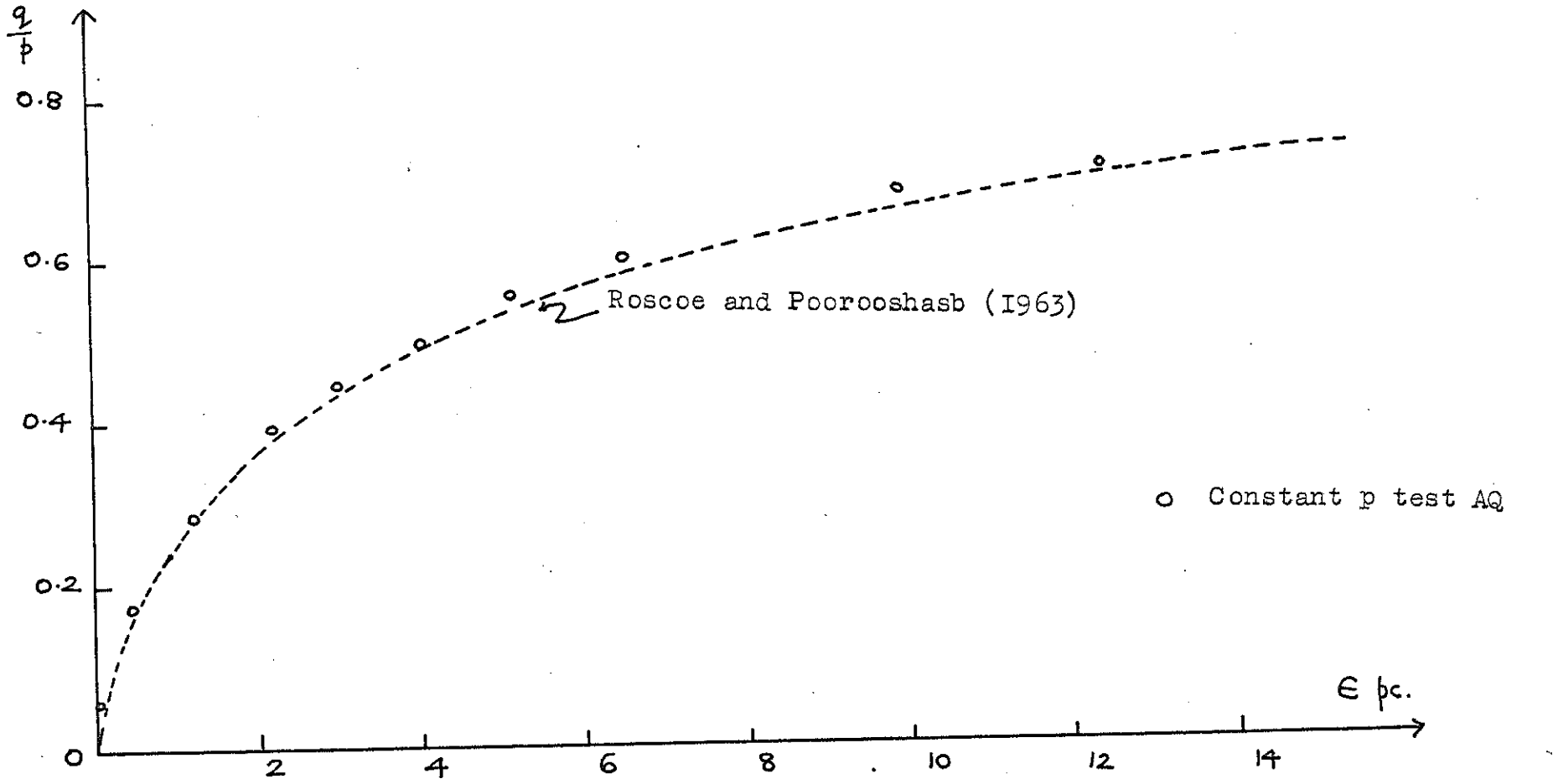

Fig.6.25. Observed and predicted ($\frac{q}{p}$, ϵ) relationship for a constant p test from an isotropic stress of 60 psi.

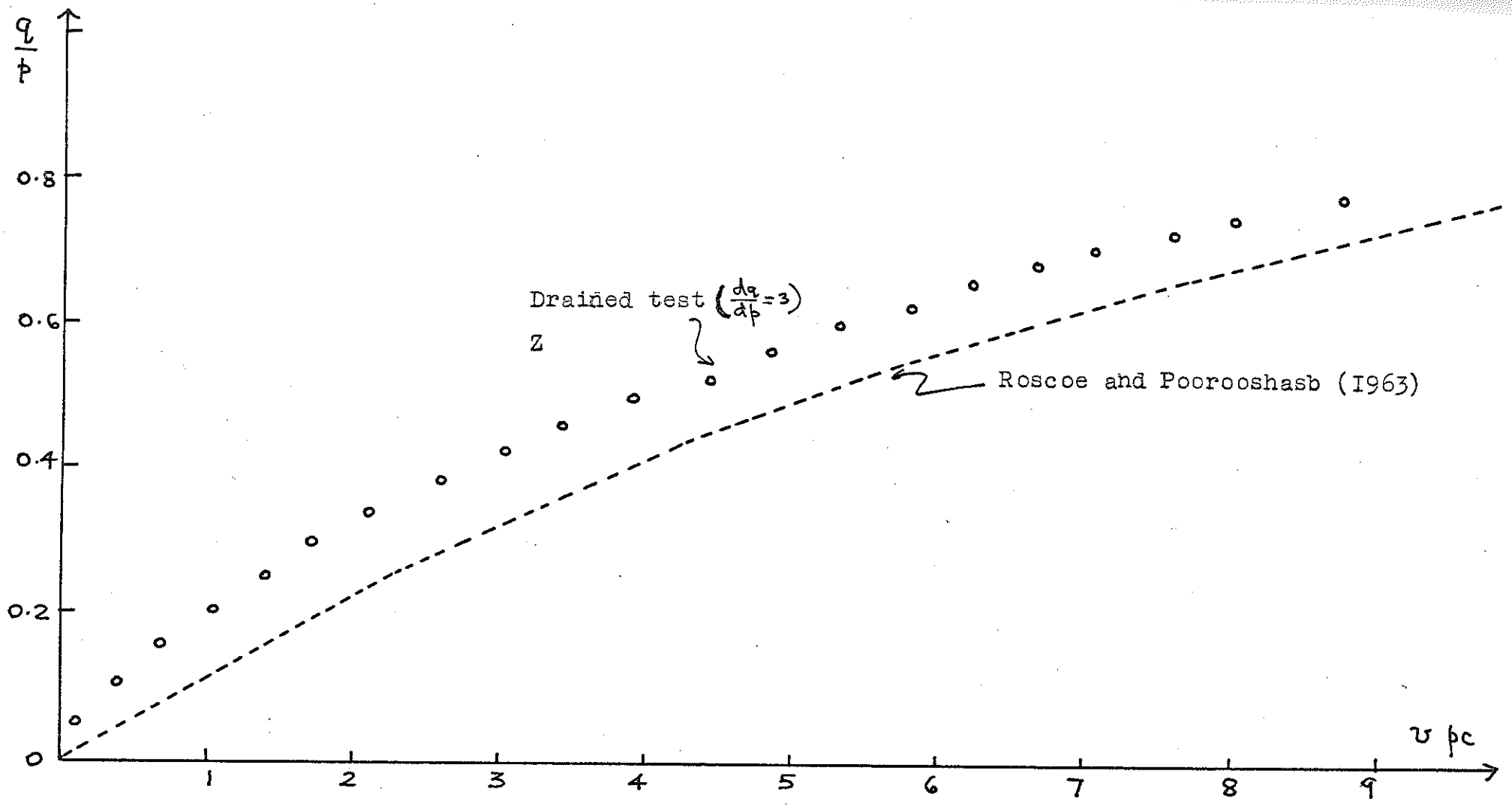

Fig. 6.26. Observed and predicted ($\frac{q}{p}$, v) relationship for a fully drained test from 60 psi isotropic stress with constant cell pressure.

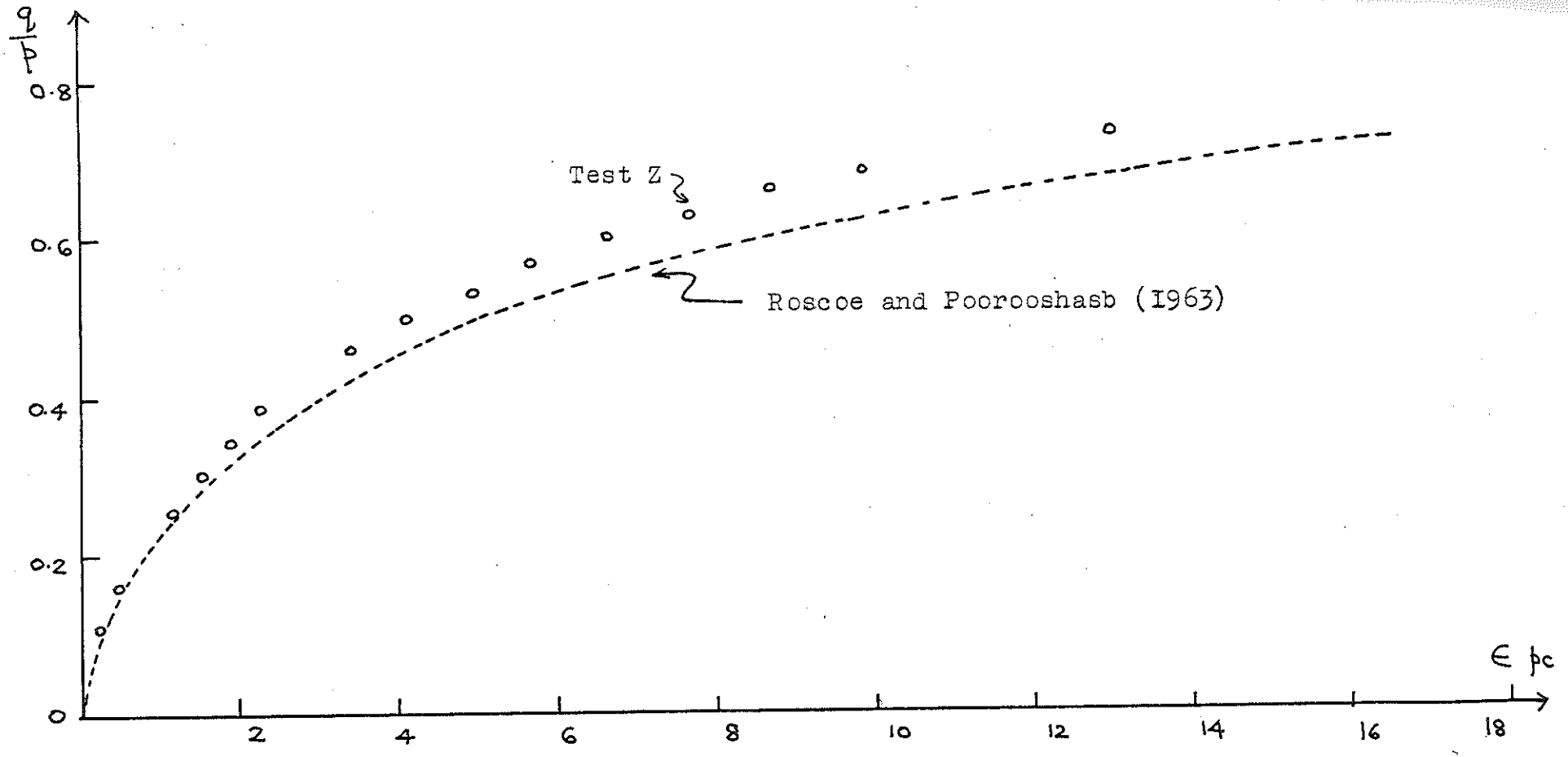

Fig. 6.27. Observed and predicted ($\frac{q}{p}$, ϵ) relationship for a fully drained test from 60 psi isotropic stress with constant cell pressure.

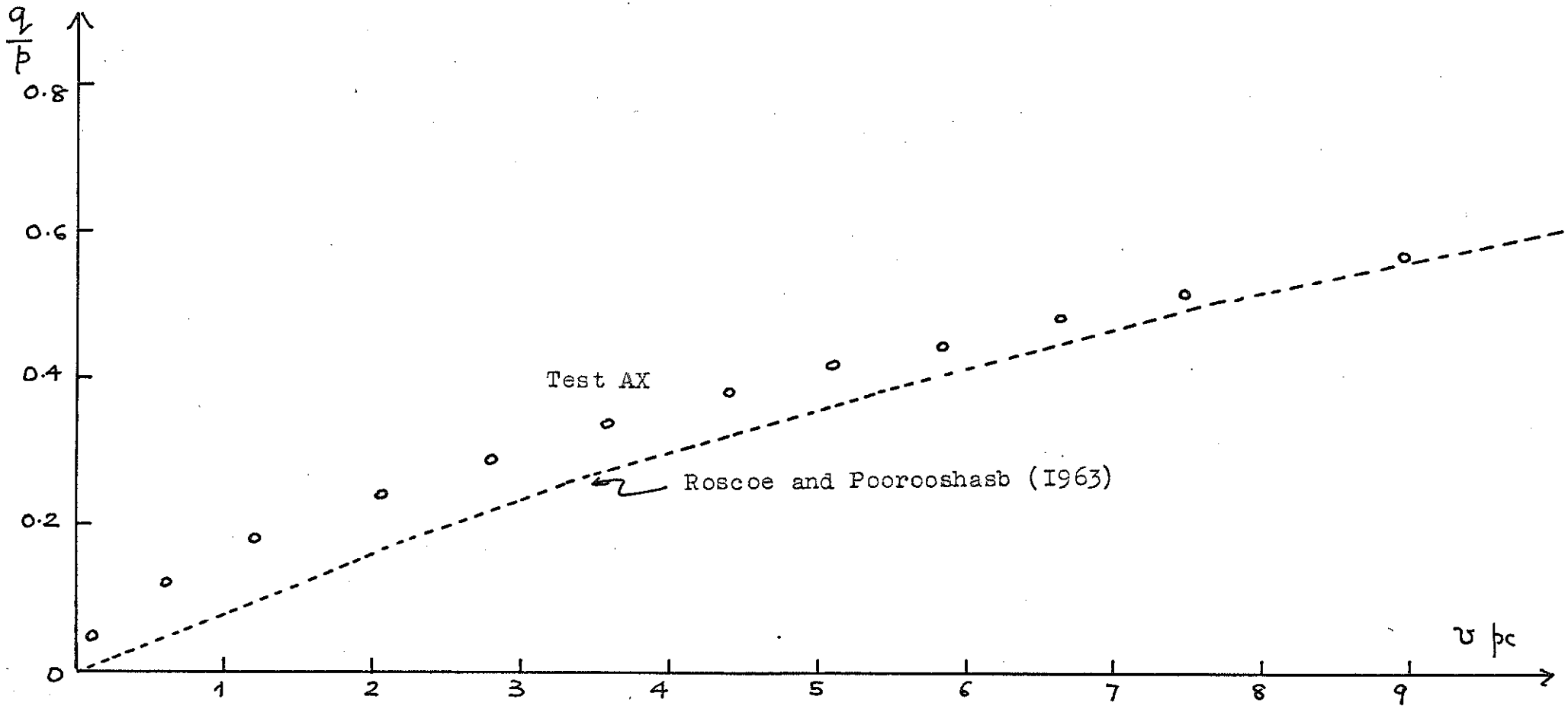

Fig. 6.28. Observed and predicted (q/p, v) relationship for a drained test from 60 psi isotropic stress with applied stress path of slope I.5

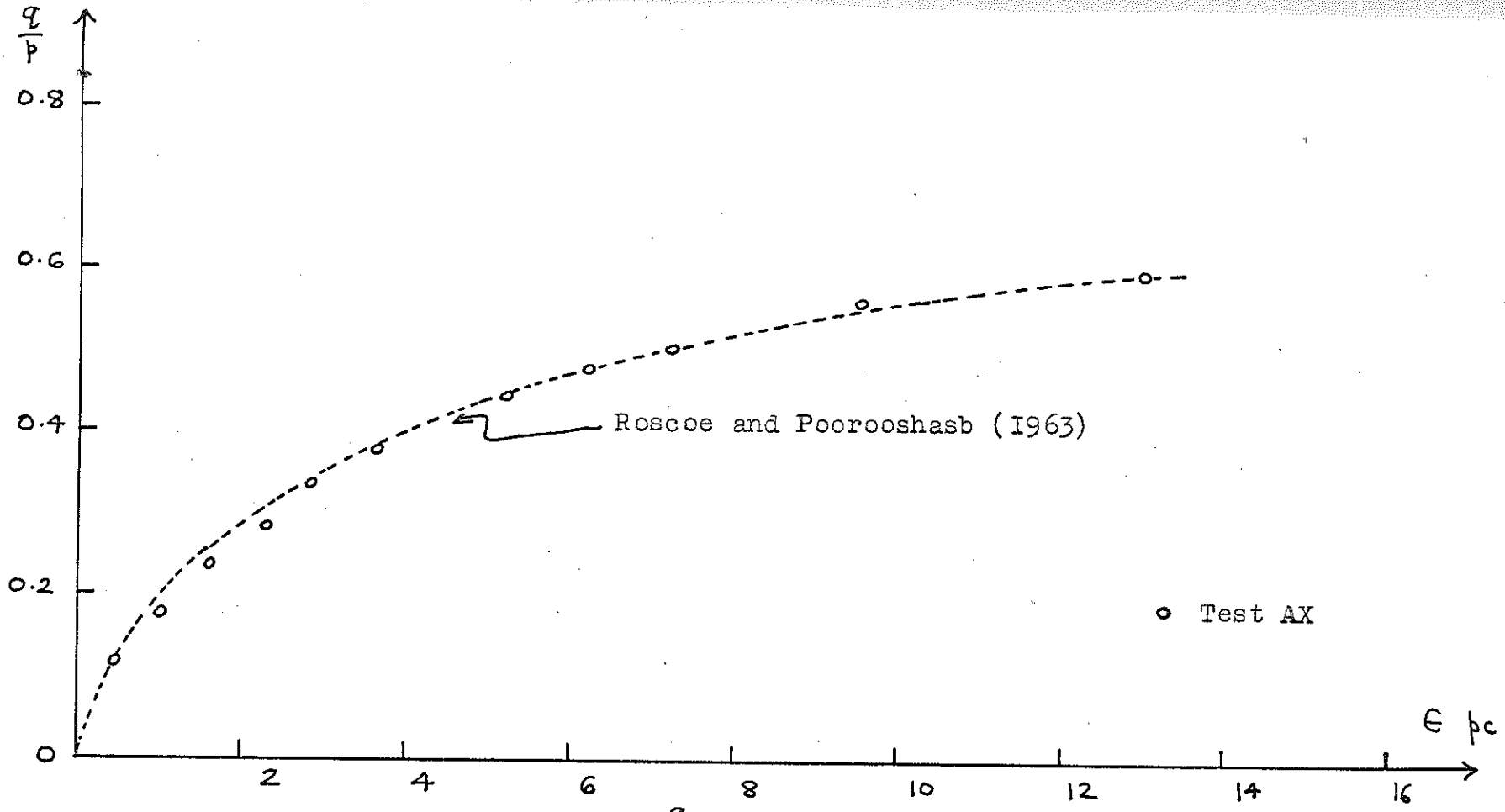

Fig. 6.29. Observed and predicted (q/p, ϵ) relationship for a drained test from 60 psi isotropic stress with an applied stress path of slpoe I.5.

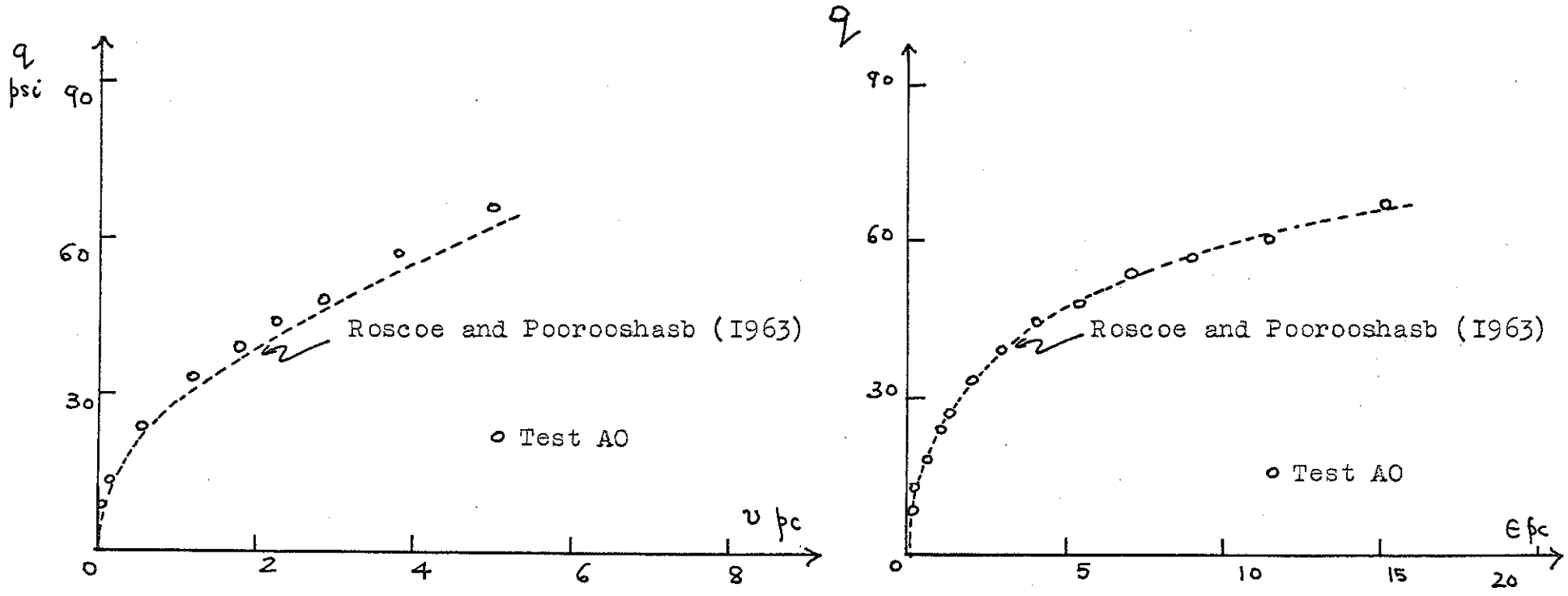

Fig. 6.30. Observed and predicted (q, υ) and (q, ϵ) relationships for a constant p test from an isotropic stress of 90psi.

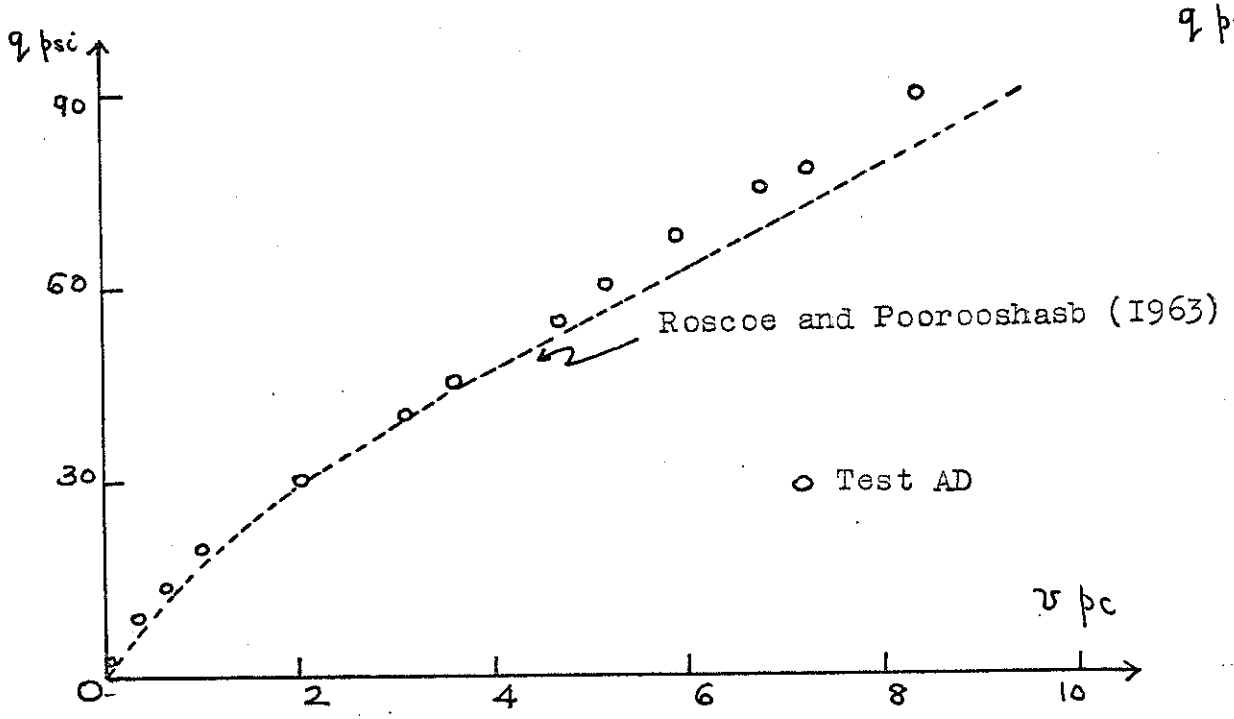

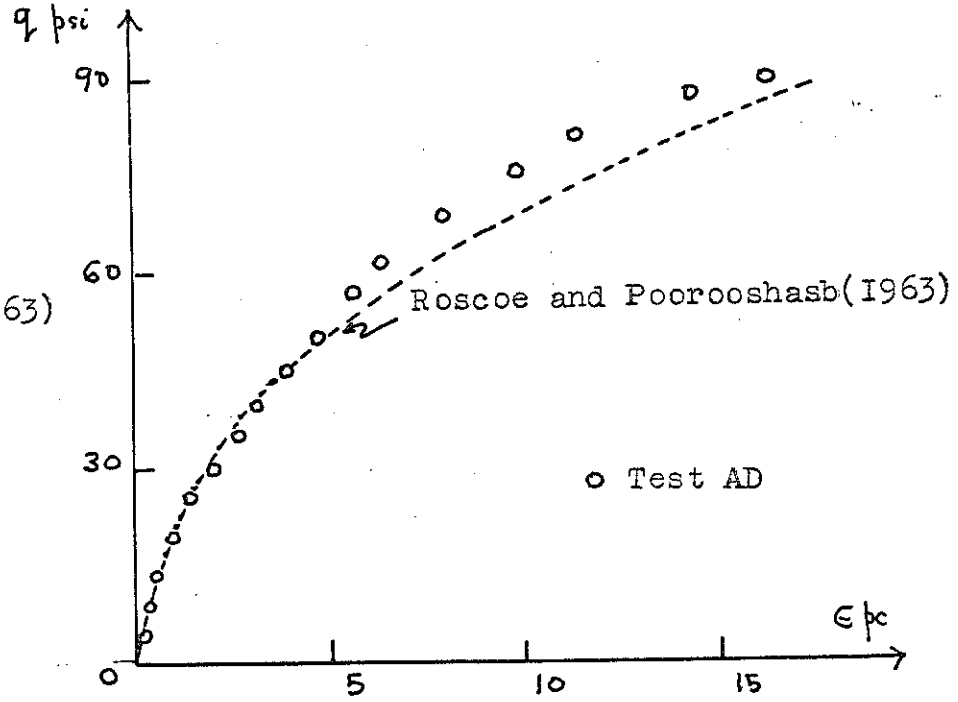

Fig. 6.31. Observed and predicted (q, v) and (q, ϵ) relationships for a fully drained test from 90 psi isotropic stress with constant cell pressure.

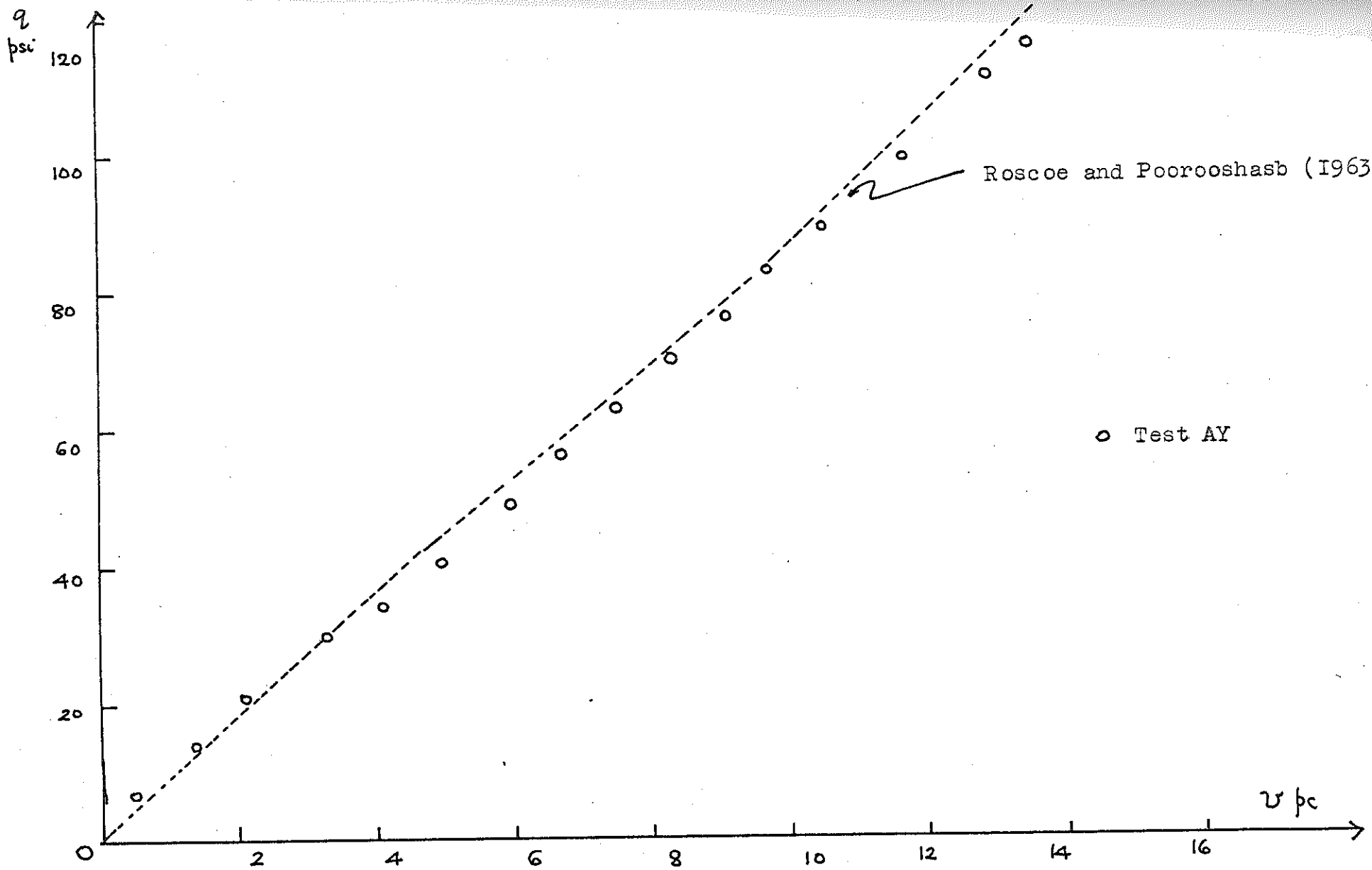

Fig. 6.32. Observed and predicted strains for a drained test with applied stress path of slope 1.5